Pergamon

PII S0016-7037(02)01141-9

Thermodynamic description of aqueous nonelectrolytes at infinite dilution over a wide range of state parameters

NIKOLAY N. AKINFIEV[1,2,*,†] and LARRYN W. DIAMOND[2†]

[1]Department of Chemistry, Moscow State Geological Prospecting University, Miklukho-Maklai str. 23, Moscow 117873, Russia
[2]Institute of Geological Sciences, University of Leoben, Peter-Tunner-Strasse 5, A-8700 Leoben, Austria

Abstract—A new, virial-like equation of state (EoS) for describing the thermodynamic properties of aqueous nonelectrolytes at infinite dilution is proposed. It is based on the accurate EoS for a solvent (H_2O) given by Hill (1990) and requires only three empirical parameters to be fitted to experimental data, and these are independent of temperature and pressure. Knowledge of the thermodynamic properties of a pure gas, together with these three parameters, enables prediction of the whole set thermodynamic properties of the solute at infinite dilution (chemical potential, entropy, molar volume, and apparent molar heat capacity) over a wide range of temperatures (0 to 500°C) and pressures (1 to 2000 bars), including the near-critical region. In the cases in which experimental thermodynamic data are lacking, the empirical parameters can be estimated solely from the known standard-state properties of the solute. The new EoS is compatible with the Helgeson-Kirkham-Flowers model for aqueous electrolytes, and thus it can be applied to reactions involving minerals, gases, and aqueous ions, in addition to uncharged species. *Copyright © 2003 Elsevier Science Ltd*

1. INTRODUCTION

Nonelectrolytes, i.e., neutral (uncharged) chemical species, are just as important in aqueous fluids in the Earth's crust as their ionic (charged) brethren. Hydrothermal, metamorphic, and diagenetic fluids often contain considerable amounts of neutral species such as CO_2, CH_4, N_2, NH_3, SO_2, and H_2S. Minor but significant nonelectrolyte constituents include H_2, O_2, CO, H_3BO_3, SiO_2, light hydrocarbons, and the noble gases. Many of these species play a role in fluid-rock interactions by controlling mineral solubilities, oxidation states and, via their dissociation, bulk acidity. Nonelectrolytes also have profound effects on the pressure-temperature stability and mobility of aqueous fluids in the crust. For example, the concentration of nonelectrolytes may determine when and where fluids will boil or condense, and they contribute to determining bulk fluid properties such as density, heat capacity, wetting characteristics, and viscosity, which are relevant to processes of fluid migration.

The view of specific chemical constituents as being either electrolytes or nonelectrolytes is not clear cut, and it depends to a large extent on the pressure and temperature of the solution of interest. For example, HF and HCl are eminently strong electrolytes at ambient conditions, but under high temperatures at elevated pressures in the crust, molecular association is favoured, and even HF and HCl are dominantly present in aqueous solution as neutral species.

Because of their geochemical importance, the thermodynamic properties of aqueous nonelectrolytes must be known over a wide pressure-temperature range, and here is where the distinction between electrolytes and nonelectrolytes becomes essential. Presently available thermodynamic descriptions of

nonelectrolytes are far less accurate than those of ionic species. For instance, the well-known Helgeson-Kirkham-Flowers (HKF) equation of state (EoS) of Tanger and Helgeson (1988) provides excellent predictions of thermodynamic properties of aqueous ions over a wide range of conditions (0 to 600°C, 1 to 5000 bars). However, when extended to neutral aqueous species (Shock et al., 1989; Schulte et al., 2001), the HKF model does not predict the behaviour of nonelectrolyte solutes correctly in the near-critical and supercritical regions of water (Plyasunov, 1991; O'Connell et al., 1996; Plyasunov and Shock, 2001b).

This general deficiency is one of the reasons for the recent activity in the development of alternative EoS for aqueous nonelectrolytes (e.g., Harvey, 1996; O'Connell et al., 1996; Majer, 1999; Plyasunov et al., 2000a, 2000b; Sedlbauer et al., 2000). The study presented here is one such attempt. We propose a simple, low-parametric EoS for aqueous nonelectrolytes that is valid for a wide range of state parameters spanning ambient, near-critical, and supercritical conditions.

In this paper, we describe the theoretical basis for the new model; we then test its capacity to reproduce existing experimental data for the species CO_2, CH_4, H_2, H_2S, NH_3, Ar, H_3BO_3, HF, and C_6H_6; and we briefly compare its performance to other equations of state. The detailed derivation of the equation is given in the Appendix. We demonstrate that although our equation contains only three empirical parameters, it performs as well as other multiparameter equations. The simplicity of our approach thus promises potential for development of highly accurate equations and eventually for incorporation of electrolyte species.

2. BASIC RELATIONS

Because many of the nonelectrolytes of geochemical interest are gases when pure under ambient conditions, the thermodynamic treatment of aqueous nonelectrolytes is often based on the well-known formalism for dissolved "gas" species. How-

---

* Author to whom correspondence should be addressed (akinfiev@geo.unibern.ch).
† *Present address:* Institute of Geological Sciences, University of Bern, Baltzerstrasse 1-3, CH-3012 Bern, Switzerland.

ever, this choice does not exclude modeling the dissolution of liquids or solids. If we consider a binary mixture in which H_2O is the solvent (component 1) and in which a dissolved nonelectrolyte is the solute ("gas" component 2), then at a given pressure P (bars) and temperature T (K), the chemical potential of the solute, $\mu_2(P,T)$, is conventionally expressed as

$$\mu_2(P,T) = \mu_g^\circ(T) + \tilde{R}T \ln f_2(P,T). \quad (1)$$

In this expression, $\mu_g^\circ(T)$ is the chemical potential of the pure gas (cal $\cdot$ mol^{-1}) at standard pressure (1 bar), $\tilde{R} = 1.9872$ cal $\cdot$ mol$^{-1} \cdot$ K^{-1} is the gas constant, and f_2 (in bars) is the fugacity of the gas in the mixture, where

$$f_2(P,T) = P \cdot \varphi_2(P,T) \cdot x_2. \quad (2)$$

Here, φ_2 is the fugacity coefficient of the solute, and x_2 is the amount-of-substance fraction (commonly termed *mole fraction*) in the mixture. Knowledge of the equations of state for pure components, together with various mixing rules (e.g., Beattie, 1955; Wong and Sandler, 1992), enables φ_2 to be estimated. For example, the two-parameter EoS of Redlich and Kwong (1949) and its modifications are widely used for predicting phase and activity relations for H_2O mixtures with CO_2, H_2, CH_4, and other components that are important for geochemical and technical applications (e.g., Ferry and Baumgartner, 1987).

Nevertheless, there are some intrinsic restrictions on applying the modified Redlich-Kwong approach. First, it fails in the low-temperature region, where liquid H_2O is strongly nonideal, and second, it yields inaccurate predictions for concentrations close to infinite dilution ($x_2 \rightarrow 0$), at which solute-solvent intermolecular interactions dominate.

To avoid the latter difficulty, another standard state for the solute is commonly used, namely, unit molality. In this case, the chemical potential of the dissolved component 2 can be written as

$$\mu_2 = \mu_{2,aq}^\circ(P,T) + \tilde{R}T \ln a_2 = \mu_{2,aq}^\circ(P,T) + \tilde{R}T \ln m_2$$
$$+ \tilde{R}T \ln \gamma_{2,m}. \quad (3)$$

Here, $\mu_{2,aq}^\circ(P,T)$ stands for the standard molar chemical potential of component 2 at unit molality (1 mol $\cdot$ kg^{-1} H_2O), which automatically takes account of close-range molecular interactions; a_2 is the activity of component 2 in aqueous solution, such that $a_2 = m_2 \cdot \gamma_{2,m}$; m_2 is the molality; and $\gamma_{2,m}$ is the corresponding activity coefficient in molality notation.

On the basis of Eqn. 1 to 3, we can write the thermodynamic equilibrium constant for the gas dissolution reaction, $A_{gas} \Leftrightarrow A_{aq}$, as

$$\ln K^\circ \equiv -\frac{\mu_{2,aq}^\circ - \mu_g^\circ}{\tilde{R}T} = \ln \frac{m_2 \cdot \gamma_{2,m}}{P\varphi_2 \cdot x_2}. \quad (4)$$

In the case of infinite dilution, when $m_2 \rightarrow 0$, then $\gamma_{2,m} \rightarrow 1$. At the same time, for a binary mixture, $x_2 \rightarrow m_2/N_w$, where $N_w = 1000/M_w \approx 55.51$ mol, and M_w denotes the molar mass of H_2O (18.0152 g $\cdot$ mol^{-1}). Defining the fugacity coefficient of the solute at infinite dilution as $\varphi_2^\infty \equiv \varphi_2|_{m_2 \rightarrow 0}$, we finally obtain

$$\ln K^\circ \equiv -\frac{\mu_{2,aq}^\circ - \mu_g^\circ}{\tilde{R}T} = \ln \frac{N_w}{P \cdot \varphi_2^\infty}. \quad (5)$$

Gas solubilities are often expressed in terms of Henry's law constants, k_H. The relation between k_H (bars) and K° can be expressed as (Prausnitz et al., 1986)

$$k_H = \frac{N_w}{K^\circ}. \quad (6)$$

Now, combining Eqn. 5 and 6, we can write

$$\ln k_H = \ln(\varphi_2^\infty \cdot P). \quad (7)$$

Various multiparameter P-T dependencies for $\mu_{2,aq}^\circ$ or for k_H have been proposed in the literature (Barta and Bradley, 1985; Levelt Sengers et al., 1986; Shock et al., 1989; Levelt Sengers and Gallagher, 1990; O'Connell et al., 1996; Plyasunov et al., 2000a, 2000b; Sedlbauer et al., 2000; see also the recent review by Sedlbauer and Majer, 2000). In our previous study (Akinfiev, 1997), the Redlich-Kwong EoS was extended to describe φ_2^∞ down to 100°C. This extension was essentially based on the exact multiparameter, unified EoS for H_2O published by Hill (1990). Now, building on this approach, we propose a simpler, low-parametric description based on the virial EoS. This new formulation is applicable over a wide temperature-pressure range, including the H_2O critical region.

In its simplest form, the virial EoS for a pure gas can be written as

$$\frac{PV}{RT} = 1 + \frac{B(T)}{V} = 1 + B_\rho(T)\rho, \quad (8)$$

where V is the molar volume (cm$^3 \cdot$ mol^{-1}) at temperature T (K) and pressure P (bars), $R = 83.1441$ cm$^3 \cdot$ bar $\cdot$ K$^{-1} \cdot$ mol^{-1} is the gas constant, ρ is the density of the gas (g $\cdot$ cm^{-3}), and $B(T)$ (cm$^3 \cdot$ mol^{-1}) or $B_\rho(T)$ (cm$^3 \cdot$ g^{-1}) corresponds to the second virial coefficient in terms of volume V or density ρ, respectively. The alternative forms of this coefficient are related simply by $B = B_\rho \cdot M$, where M is the molar mass of the gas (g $\cdot$ mol^{-1}). Statistical thermodynamics shows that the second virial coefficient B has a well-defined physical meaning in that it is unambiguously related to the intermolecular interaction energy (e.g., Mason and Spurling, 1970).

The fugacity of the gas can now be derived by integration of Eqn. 8 using standard procedures (see, e.g., Prausnitz et al., 1986. Details of the derivation of the formulas are given in the Appendix). As a result, the fugacity coefficient of the solute at infinite dilution can be expressed as

$$\ln \varphi_2^\infty = \frac{2}{V_1^\circ} B_{12} - \ln \frac{RT}{PV_1^\circ}. \quad (9)$$

Here, B_{12} stands for a virial cross-coefficient that characterizes interaction between the dissimilar molecules of the solute and the solvent, and V_1° denotes the molar volume of the pure solvent. Evidently, to describe φ_2^∞ (or k_H) over a wide range of geochemical conditions, we must know the dependence of B_{12} on P and T. The description of this function, in the simplest way possible, is the principal task of our study.

Before outlining the development our equation below, we point out three special aspects of our approach that should be borne in mind:

1. Whereas the "traditional" formulation of the virial equation (Eqn. 8) assumes that the second virial coefficient is independent of pressure and density (i.e., B is a function of T only), our formulation treats B as a function of both P and T.

2. Because of the different functional dependency of our B parameter, its values differ significantly from those of the "traditional" second virial coefficients. Thus, to avoid any confusion, the term *virial* will no longer be used when referring to our B parameters below. It is nonetheless important to realise that our B parameters maintain their physical meaning as measures of close-range interactions between molecules.

3. We assign the equations for fugacity coefficients (Eqn. 9, A5, and A7) the role of empirical master equations. Thus, we do not use Eqn. 8 to describe volumes. Instead, we use accurate derivatives of Eqn. 9 to obtain all required thermodynamic properties.

3. DEVELOPMENT OF THE NEW EOS

The essential step of our approach is to find empirical P-T dependencies not directly for B_{12} but with respect to the known B values of the solvent. The simplest route to this end is to use an expression analogous to Eqn. 9 for the fugacity coefficient of the pure solvent (see the Appendix):

$$\ln\varphi_1^\circ = \frac{2}{V_1^\circ} B_1 - \ln\frac{RT}{PV_1^\circ}, \tag{10}$$

where B_1 denotes the solvent-solvent interaction parameter for pure H_2O. Now, subtracting Eqn. 10 from Eqn. 9 and taking into account Eqn. 7, we obtain

$$\ln k_H = \ln(\varphi_1^\circ \cdot P) + \frac{2}{V_1^\circ}(B_{12} - B_1) = \ln f_1^\circ + \frac{2}{V_1^\circ}\Delta B, \tag{11}$$

or, in terms of density

$$\ln k_H = \ln f_1^\circ + 2\Delta B_\rho \cdot \rho_1^\circ. \tag{12}$$

Here, $f_1^\circ \equiv \varphi_1^\circ P$ and ρ_1° are the fugacity (bars) and density (g · cm^{-3}) of the pure solvent (H_2O) at given P-T conditions, and $\Delta B \equiv B_{12} - B_1$ (cm^3 · mol^{-1}) stands for the difference in interaction between dissimilar molecules vs. that between identical solvent molecules, and $\Delta B = \Delta B_\rho \cdot M$.

Eqn. 12 lends itself to modeling the numerous experimental data on k_H for various dissolved gases at different temperatures (Ar: Crovetto et al., 1982; Namiot, 1991; CH$_4$: Namiot, 1979; Crovetto et al., 1982; Cramer, 1984a; CO$_2$: Malinin, 1979; Carroll et al., 1991; Crovetto, 1991; Plyasunov and Zakirov, 1991; Crovetto and Wood, 1992; Gallagher et al., 1993; N$_2$: Alvarez et al., 1988; Namiot, 1991; H$_2$: Kishima and Sakai, 1984; Alvarez et al., 1988; Namiot, 1991; H$_2$S: Kozintseva, 1964; Clarke and Glew, 1971; Drummond, 1981; Kishima, 1989; Suleimenov and Krupp, 1994; O$_2$: Cramer, 1984b; Namiot, 1991; NH$_3$: Jones, 1963; Kawazuishi and Prausnitz, 1987).

Japas and Levelt Sengers (1989) pointed out that values of $T\ln(k_H/f_1^\circ)$ for many aqueous solutes show linear behaviour over a wide temperature range when plotted against H_2O density, ρ_1°:

$$T\ln(k_H/f_1^\circ) = \alpha + \beta \cdot \rho_1^\circ. \tag{13}$$

This observation justifies the unified description of dissolved gases using only two empirical parameters (Harvey and Levelt Sengers, 1990; Levelt Sengers and Gallagher, 1990). Unfortunately, despite the appealing simplicity of this approximation, it does not produce the correct asymptotic behaviour for an ideal gas of $k_H \to f_2^\circ$ as $\rho_1^\circ \to 0$ and $f_2^\circ \to f_1^\circ$ when $\alpha \neq 0$ (Plyasunov et al., 2000a). Moreover, Eqn. 13 does not work properly at low temperatures ($T < 100°C$).

To find a more appropriate dependency, we have tested various two- and three-parameter formulations of $\Delta B_\rho(T, \rho_1^\circ)$ using all available experimental data on k_H for the above-mentioned dissolved gases, such that

$$2\Delta B_\rho(T, \rho_1^\circ) = \frac{1}{\rho_1^\circ}\ln\left(\frac{k_H}{f_1^\circ}\right). \tag{14}$$

We note that the data for CO_2, H_2, and H_2S cover the supercritical region as well. It was found that the best fit within the group of two-parameter equations is given by the approximation

$$2\Delta B_\rho = a + b\left(\frac{10^3}{T}\right)^{0.5}. \tag{15}$$

Here, a (cm^3 · g^{-1}) and b (cm^3 · K$^{0.5}$ · g^{-1}) denote the adjustable parameters. In comparison to Eqn. 13, the linearity of Eqn. 15 extends into the low-temperature region, and thus, the restrictions of Eqn. 13 are overcome. The application of Eqn. 12 together with Eqn. 15 provides good prediction of k_H values over the entire temperature range of interest, and the maximum error does not exceed 0.2 log units. Nevertheless, derivatives of Eqn. 12 with respect to pressure and temperature result in lower accuracy. CO_2 serves as an example of this fact. Although the molar volumes of dissolved CO_2 show the proper tendency at high temperatures when calculated with Eqn. 12 and 15 using a and b parameters retrieved from the k_H data, the values for $T < 100°C$ show large discrepancies of $\sim$3 to 7 cm^3 · mol^{-1} (20 to 40%). Our tests demonstrated that use of other kinds of approximations instead of Eqn. 15, or of three-parameter equations, does not alter the fit significantly. Therefore, it proved necessary to introduce an auxiliary parameter to better describe the volume of the dissolved molecule.

The simplest way to do this is to "compare" Eqn. 9 for $\ln\varphi_2^\infty$ not directly with Eqn. 10 for pure H_2O but with a "scaled H_2O molecule," increased in size by $(1 - \xi)$ times (ξ being a dimensionless, empirically fitted factor, as introduced by Plyasunov et al., 2000a). Thus, we multiply Eqn. 10 by $(1 - \xi)$ and then subtract it from Eqn. 9. Instead of Eqn. 11, we now obtain

$$\ln k_H = (1 - \xi) \cdot \ln f_1^\circ \xi \ln\frac{RT}{V_1^\circ} + \frac{2}{V_1^\circ}\Delta B, \tag{16}$$

or, in terms of density

$$\ln k_{\mathrm{H}} = (1 - \xi) \cdot \ln f_1^\circ + \xi \ln\left(\frac{RT}{M_w} \cdot \rho_1^\circ\right) + 2\rho_1^\circ \cdot \Delta B_\rho.$$
(17)

Here again, M_w denotes the molar mass of H_2O, $\Delta B = \Delta B_\rho \cdot M_w$, ξ is the empirical scaling factor, and $\Delta B \equiv B_{12} - (1 - \xi) \cdot B_1$ stands for the difference in interaction between dissimilar molecules vs. that between "scaled" pure solvent molecules. It can be seen that if component 2 is set to be identical to H_2O, then $\xi = 0$, and Eqn. 17 reverts to Eqn. 12. In other cases, ξ may be $>$ or < 0.

Taking into account Eqn. 5 and 6, we can now rewrite Eqn. 17 in the appropriate form for the chemical potential of the dissolved component:

$$\mu_{2,\mathrm{aq}}^\circ(P,T) = \mu_\mathrm{g}^\circ(T) - \tilde{R}T \ln N_w + (1 - \xi)\tilde{R}T \ln f_1^\circ$$
$$+ \tilde{R}T\xi\ln\left(\frac{RT}{M_w}\rho_1^\circ\right) + \tilde{R}\left\{T\rho_1^\circ \cdot \left[a + b\left(\frac{10^3}{T}\right)^{0.5}\right]\right\}. \quad (18)$$

Thus, our EoS (Eqn. 18) contains three empirical constants that are independent of pressure and temperature: a "scaling" factor ξ and two others (a and b) to account for the temperature dependence of ΔB_ρ (Eqn. 15). Eqn. 18 yields the correct low-density limit for all thermodynamic properties of the solute (see the Appendix), as noted for similar equations by Plyasunov et al. (2000a).

Derivatives of Eqn. 18 with respect to pressure and temperature provide the relations for partial molar volume, entropy, and heat capacity of the dissolved component, as follows:

$$V_2^\circ \equiv \left.\frac{\partial \mu_{\mathrm{aq}}^\circ}{\partial P}\right|_T = V_1^\circ(1 - \xi) + \xi RT \frac{1}{\rho_1^\circ}\frac{\partial \rho_1^\circ}{\partial P} + R\frac{\partial}{\partial P}\left\{T\rho_1^\circ\left[a\right.\right.$$
$$\left.\left. + b\left(\frac{10^3}{T}\right)^{0.5}\right]\right\}. \quad (19)$$

$$S_{2,\mathrm{aq}}^\circ \equiv -\left.\frac{\partial \mu_{\mathrm{aq}}^\circ}{\partial T}\right|_P = S_{2,\mathrm{g}}^\circ + (1 - \xi)(S_1^\circ - S_{1,\mathrm{g}}^\circ) + \tilde{R}\ln N_w$$
$$- \tilde{R}\left(\xi + \xi\ln\frac{RT}{M_w} + \xi\ln\rho_1^\circ + \xi T\frac{1}{\rho_1^\circ}\frac{\partial \rho_1^\circ}{\partial T}\right) - \tilde{R}\frac{\partial}{\partial T}\left\{T\rho_1^\circ\right.$$
$$\left.\left[a + b\left(\frac{10^3}{T}\right)^{0.5}\right]\right\}. \quad (20)$$

$$C_{p2}^\circ \equiv -T^2\left.\frac{\partial^2 \mu_{\mathrm{aq}}^\circ}{\partial T^2}\right|_P = C_{p2,\mathrm{g}}^\circ + (1 - \xi)(C_{p1}^\circ - C_{p1,\mathrm{g}}^\circ)$$
$$- \tilde{R}\left(\xi + 2\xi T\frac{1}{\rho_1^\circ}\frac{\partial \rho_1^\circ}{\partial T} - \xi\frac{T^2}{(\rho_1^\circ)^2}\left(\frac{\partial \rho_1^\circ}{\partial T}\right)^2 + \xi\frac{T^2}{\rho_1^\circ}\frac{\partial^2 \rho_1^\circ}{\partial T^2}\right)$$
$$- \tilde{R}T\frac{\partial^2}{\partial T^2}\left\{T\rho_1^\circ\left[a + b\left(\frac{10^3}{T}\right)^{0.5}\right]\right\}. \quad (21)$$

Here, as above, subscript g denotes the ideal gaseous component at a given temperature and standard pressure; indexes 2 and 1 stand for the dissolved component and the solvent (H_2O), respectively; and $\tilde{R} = 1.9872 \text{ cal} \cdot \text{mol}^{-1} \cdot \text{K}^{-1}$ and $R = 83.1441 \text{ cm}^3 \cdot \text{bar} \cdot \text{mol}^{-1} \cdot \text{K}^{-1}$ are the gas constant expressed in "energy" and "volume" units, respectively. The Appendix

(Eqn. A12 to A14) gives the analytical expressions for derivatives of $T\rho_1^\circ\left[a + b\left(\frac{10^3}{T}\right)^{0.5}\right]$ in Eqn. 19 to 21 with respect to pressure and temperature.

Calculation of thermodynamic properties of the dissolved species using Eqn. 18 to 21 is extremely sensitive to the properties of the pure solvent. Thus, the properties of H_2O must be known with high accuracy over the entire range of state parameters. In this study, the thermodynamic properties of pure water were calculated using the unified EoS given by Hill (1990). Data for ideal gaseous H_2O (steam) were taken from Glushko (1981).

4. ESTIMATION OF THE EMPIRICAL PARAMETERS (ξ, A, AND B)

Having derived a modified virial-like EoS, we now describe the fitting of the three empirical constants ξ, a, and b. Experimental values of V_2° at standard-state conditions were used with available experimental data on k_{H} of the dissolved species to estimate the three empirical parameters. The estimation procedure is iterative. In the first step, the scaling factor is set to zero. The available experimental data on k_{H} at various temperatures and pressures are then used to calculate values of the a and b parameters by means of the least squares method. Using these initial a and b values, the ξ parameter is calculated on the basis of the known partial molar volume of the solute (V_2°) at standard-state conditions (25°C and 1 bar) according to Eqn. 19. The resulting ξ value is then used to estimate a and b in the next iteration, and so on. This fitting procedure usually needs fewer than four iterations to reach a precision of $\approx 0.03 \text{ cm}^3 \cdot \text{mol}^{-1}$ for V_2° at 25°C and 1 bar. The quality of the fit for some dissolved gases is illustrated in Figures 1 to 3, and the retrieved empirical parameters are given in Table 1.

The empirical parameters could be easily estimated even when high-temperature experimental data were lacking. It can be seen that Eqn. 18 to 21 and Eqn. A12 to A14 in the Appendix are linear with respect to the empirical parameters ξ, a, and b. Thus, the parameters could be readily obtained using only known standard-state $\mu_{2,\mathrm{aq}}^\circ$, $S_{2,\mathrm{aq}}^\circ$, and V_2° values of the dissolved species. The set of corresponding linear equations is given in the Appendix. An example of the application of this method is the fitting of Ar. Here, accepting the standard-state properties for both aqueous and gaseous Ar from the SUPCRT92 database (Johnson et al., 1992), we obtain the values given in Table 2. These values, when used to predict the temperature dependencies of k_{H}, V_2°, and C_{p2}° of aqueous Ar, result in reasonably accurate model extrapolations (dashed curves in Figs. 1e, 2d, and 3d). Data for other aqueous species retrieved on the basis of known standard-state properties are also given in Table 2.

The fitting procedure is of course subject to the uncertainties of the available experimental data, and choices between data-sets must be made to derive unique values for the model parameters. This dilemma is well illustrated in the case of hydrogen-sulphide. The experimentally measured values of k_{H} for H_2S diverge significantly at temperatures above 200°C (Fig. 1c). Thus, we performed two fits. In the first case, the whole set of available experimental data, including the contradictory

Table 1. Empirical parameters of the equation of state (ξ, a, b; see Eqns. 18 to 21) for a number of dissolved gas species, estimated from the experimentally determined temperature dependence of Henry's constant. Where listed, the experimental value for partial molar volume of the solute, V_2°, at standard-state conditions was used in the fitting.

Species	V_2° (cm$^3 \cdot$ mol^{-1})[a]	Source for V_2°	ξ	a (cm$^3 \cdot$ g^{-1})	b (cm$^3 \cdot$ K$^{0.5} \cdot$ g^{-1})
Ar	32.6	Moore et al. (1982)	0.0733	−8.5139	11.9210
H$_2$S[b]	34.9	Barbero et al. (1983)	−0.2102	−11.2303	12.6104
H$_2$S[c]	34.9	Barbero et al. (1983)	−0.2029	−13.4046	13.8582
O$_2$	33.2	Moore et al. (1982)	0.0260	−9.7540	12.9411
N$_2$	35.7	Moore et al. (1982)	−0.0320	−11.5380	14.6278
NH$_3$	24.4	Allred and Woolley (1981)	−0.0955	−4.7245	4.9782
H$_2$	25.2	Tiepel and Gubbins (1972)	0.3090	−8.4596	10.8301
CH$_4$	37.3	Tiepel and Gubbins (1972)	−0.1131	−11.8462	14.8615
CO$_2$	32.8	Barbero et al. (1983)	−0.0850	−8.8321	11.2684
C$_6$H$_6$			−1.1010	−21.0084	22.9340
HCl			−0.2800	11.6420	−7.4244

[a] Partial molar volume of aqueous species at 298.15 K, 1 bar.
[b] Parameters were retrieved by fitting the whole set of available experimental data on Henry's constant (see also text for explanation).
[c] Parameters were retrieved by fitting the experimental data on Henry's constant for temperatures below 200°C only (see also text for explanation).

datasets at $T > 250$°C and the supercritical data of Kishima (1989), were taken into account to retrieve the adjustable parameters of the model. The result is $\xi = -0.2102$, $a = -11.2303$, and $b = 12.6104$ (Table 1). The corresponding computations are shown as continuous curves in Figures 1c, 2b, and 3b. It can be seen that the maximum deviation from the experimental data for k_H (~0.1 lgk_H units) occurs between 150 and 220°C, but the discrepancy at ambient temperatures is also noticeable. In the second case, we fitted the data for temperatures below 200°C only (where all datasets coincide). The retrieved empirical parameters are now $\xi = -0.2029$, $a = -13.4046$, and $b = 13.8582$ (Table 1), and the calculated thermodynamic properties are shown in Figures 1c, 2b, and 3b by the dotted lines. In contrast to the previous prediction, the new calculation is in excellent agreement with the experimental data for k_H at ambient conditions. In the subcritical region ($T > 275$°C), the calculated curve closely follows the data of Suleimenov and Krupp (1994), but the supercritical data of Kishima (1989) deviate appreciably from the calculations. Moreover, for this case of fitting, the retrieved entropy value, $S_{2,aq}^\circ = 29.96$ cal $\cdot$ mol$^{-1} \cdot$ K^{-1}, matches that given by Shock et al. (1989), namely, $S_{2,aq}^\circ = 30.0$ cal $\cdot$ mol$^{-1} \cdot$ K^{-1}. Volumes and heat capacities are in satisfactory accordance with the experiments in both cases of fitting.

Although we have emphasised that standard-state properties alone are sufficient to fit the model parameters, this route is also limited by the certainty of the standard-state data. In the troublesome case of H$_2$S discussed above, a rather high uncertainty is associated with the standard molar entropy of H$_2$S$_{aq}$. For example, a change of 1 cal $\cdot$ mol$^{-1} \cdot$ K^{-1} of $S_{2,aq}^\circ$ at 25°C and 1 bar leads to a shift of 0.2 lnk_H units at 300°C and vapour-saturated water pressure, P_{sat}. This shift spans the discrepancies in the experimental data plotted in Figure 1c, thereby providing no new insight. The issue of which data set for H$_2$S is the more accurate remains unresolved from a purely theoretical point of view. Indeed, at the present state of development of our EoS, it would be premature to use it as a discriminator to evaluate the accuracy of the conflicting experimental studies.

It is interesting to test our method by attempting to describe

very large organic molecules in aqueous solution. As an example, our processing of the available experimental data on benzene solubility in pure water (Jaeger, 1923; Tsonopoulos and Wilson, 1983; Kertes, 1989; Miller and Hawthorne, 2000) yields the adjustable parameters given in Table 1. Model parameters for the same aqueous species derived from the known standard-state properties are given in Table 2. Calculated temperature dependencies of k_H, V_2°, and C_{p2}° for both cases are compared to the experimental data in Figures 4 and 5. It can be seen that in the first case, our method somewhat underestimates V_2°, but prediction of k_H and C_{p2}° is quite fair (solid curves). Moreover, the estimated entropy value of standard-state conditions ($S_{2,aq[298\,K,\,1\,bar]}^\circ = 34.48$ cal $\cdot$ mol$^{-1} \cdot$ K^{-1}) is quite close to the predicted values of 35.5 and 35.66 given by Amend and Helgeson (1997) and Plyasunov and Shock (2000), respectively. In cases in which the empirical parameters are retrieved from the known standard-state properties, the new EoS tends to overestimate the heat capacity (Table 2 and dashed curve in Fig. 5). Nevertheless, the temperature dependence of the Henry constant, k_H, (i.e., chemical potential of aqueous C$_6$H$_6$) is predicted within the experimental error.

5. DISCUSSION

The new EoS can be viewed as a development of the semiempirical approach derived by Japas and Levelt Sengers (1989). These authors adopted a linear relationship between ΔB and the reciprocal temperature, T^{-1}, whereas we have used an approximation (Eqn. 15) that provides better linearity to the T derivative of lnk_H. It is interesting to observe that Eqn. 15 is similar to Redlich and Kwong's (1949) equation, whereby the intermolecular parameter is set proportional to $T^{-0.5}$.

One of the challenges of any EoS for aqueous species is to predict correctly the behaviour of solutes near the critical point of H$_2$O. A useful indicator of such accuracy is the so-called Krichevskii parameter, A_{Kr} (Levelt Sengers, 1991):
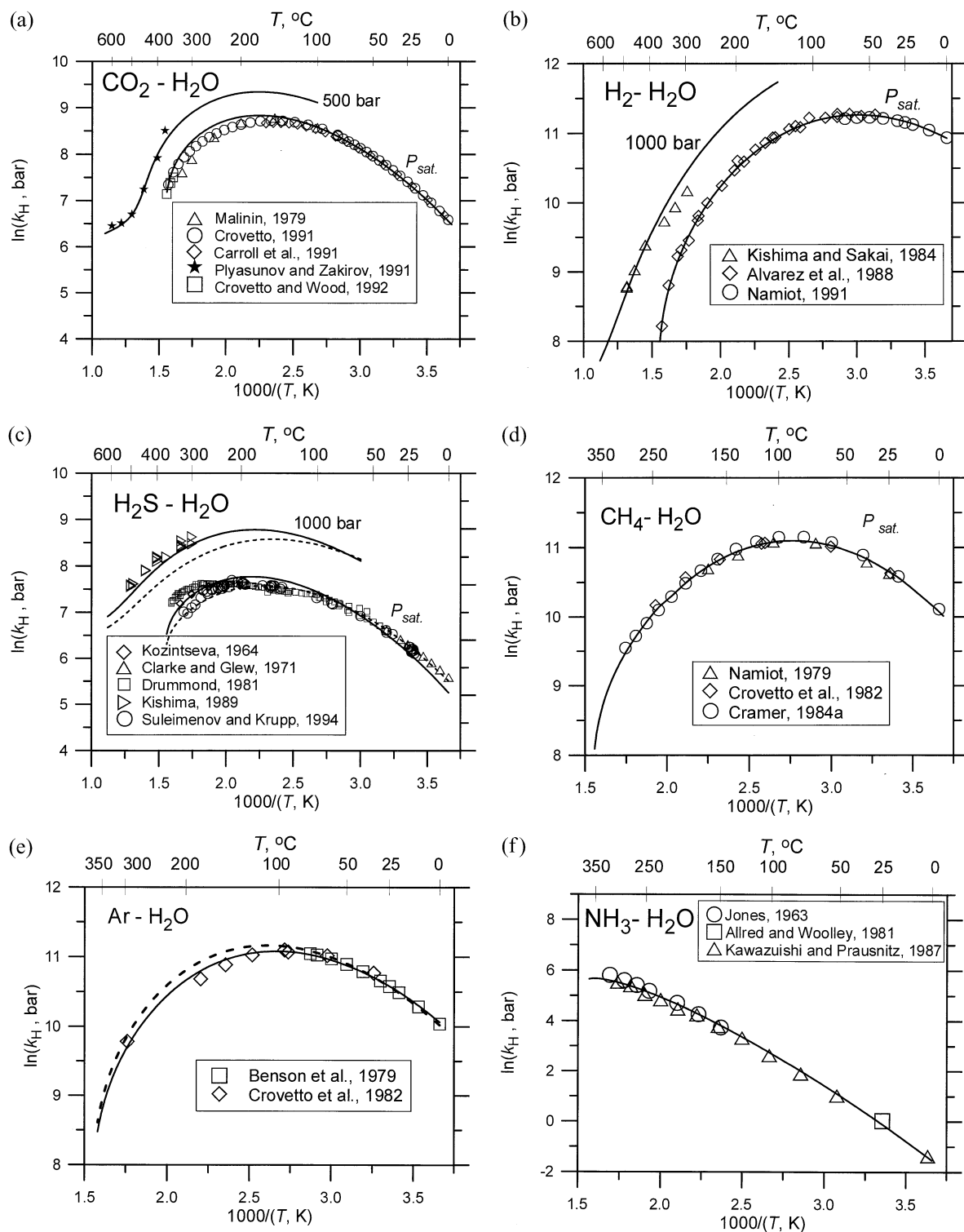
Fig. 1. Natural logarithm of Henry's constant, $\ln k_H$, for several dissolved gases at vapour-saturated water pressure (P_{sat}) and other specified pressures, plotted against reciprocal temperature. Symbols correspond to experimental data. Continuous curves are our equation of state (EoS) predictions using Eqn. 15 and 17 and data from Table 1. Dashed curves are our EoS predictions for H_2S_{aq} and Ar_{aq}, based on standard-state properties only (Table 2, see also text).
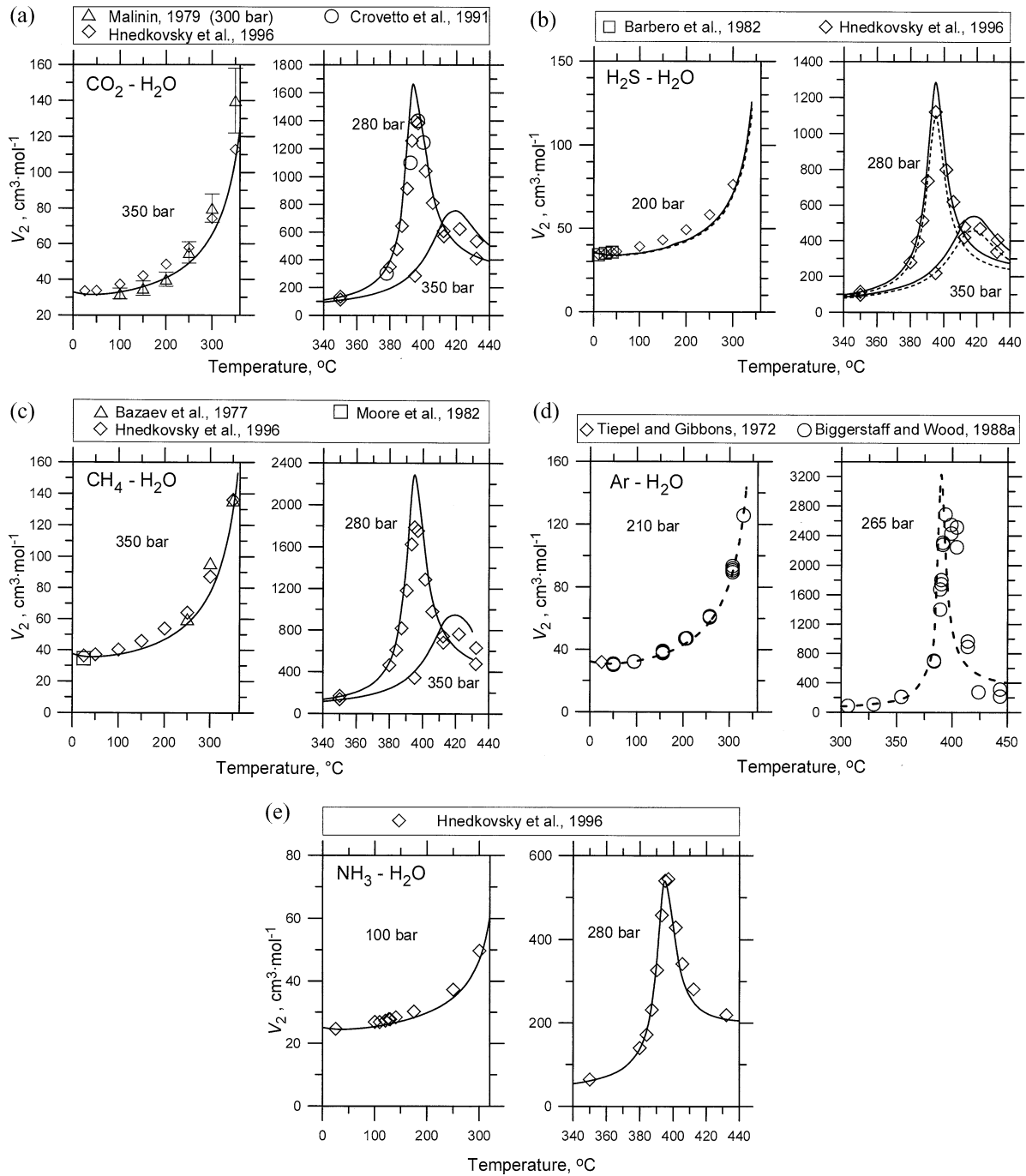
Fig. 2. Partial molar volumes of dissolved gases at subcritical (left) and supercritical (right) conditions. Symbols correspond to experimental data. Solid curves are our equation of state (EoS) predictions at infinite dilution (Eqn. 19 and A14 and parameters from Table 1). Dashed curves are our EoS predictions for H_2S_{aq} and Ar_{aq}, based on standard-state properties only (Table 2, see also text).

$$A_{Kr} = \frac{V_2^\circ}{k_T V_1^\circ}\bigg|_{cr}, \qquad (22)$$

where $k_T \equiv \frac{1}{\rho_1^\circ}\cdot\frac{\partial\rho_1^\circ}{\partial P}$ is the compressibility of pure water, and index cr indicates that the evaluation is performed at the critical point of H_2O. Although $k_T \to \infty$ as the critical point is ap-

proached, the Krichevskii parameter is finite. According to statistical mechanics and fluctuation solution theory (O'Connell, 1994), A_{Kr} reflects solute-H_2O interactions at the critical point of water. Using our equation for V_2° (Eqn. 19 and A14) at $T = T_{cr} = 647.1$ K, and $\rho_1^\circ = \rho_{1,cr}^\circ = 0.3228$ g · cm^{-3} (Hill, 1990), we obtain
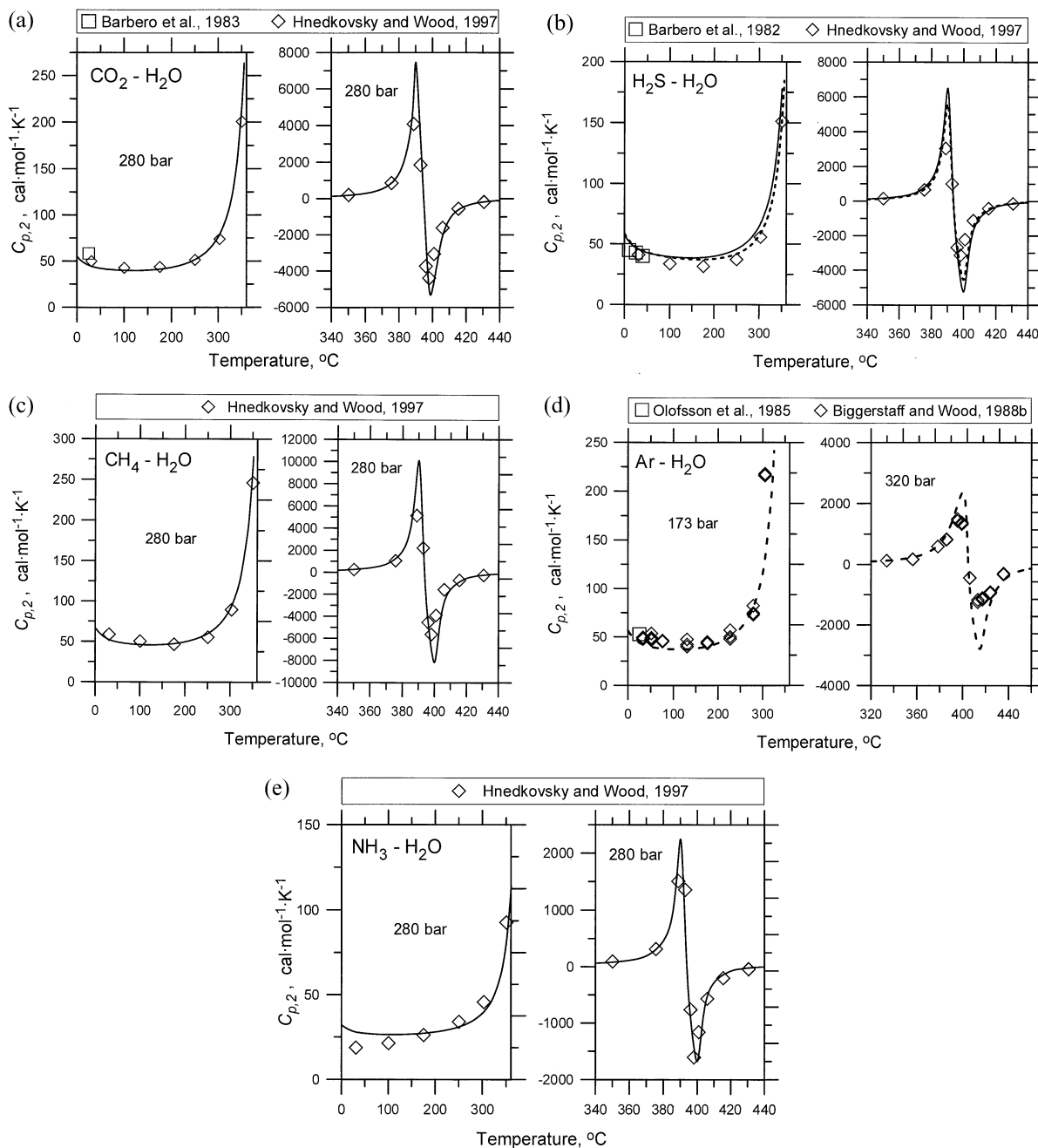
Fig. 3. Apparent molar heat capacities of dissolved gases at subcritical (left) and supercritical (right) temperatures. Symbols denote experimental data. Solid curves are our equation of state (EoS) predictions at infinite dilution and P and T of interest (Eqn. 21 and A13 and parameters from Table 1). Dashed curves are our EoS predictions for H_2S_{aq} and Ar_{aq}, based on standard-state properties only (Table 2, see also text).

$$A_{Kr} = \frac{\xi RT_{cr}}{V_{1,cr}^\circ} + \frac{RT\rho_{1,cr}^\circ \cdot 2\Delta B_\rho}{V_{1,cr}^\circ} = 963.93 \ (\xi + 0.3228 \cdot [a + b \cdot 1.2432]), \quad (23)$$

where A_{Kr} is in bars. Values calculated using Eqn. 23 with data from Tables 1 and 2 are close to those given by Plyasunov and Shock (2001a), who estimated A_{Kr} from various types of experimental information for more than 30 aqueous nonelectro-

lytes. As an example, for benzene (Table 1), we obtain $A_{Kr} = 1234$ bars, which lies within the range of 950 to 1250 bars given by Plyasunov and Shock (2001a). Our predictions for molecules based on the standard-state properties only (Table 2) are also close to those given by Plyasunov and Shock (2001a): we obtain 2086 bars for C_2H_6 and -806 bars for H_3BO_3, whereas those authors reported 1944 ± 400 and -670 ± 100 bars, respectively.

Table 2. Empirical parameters of the equation of state (ξ, a, b; see Eqns. 18 to 21) for a number of dissolved gas species, estimated from known standard-state properties only.

Species	$\mu^\circ_{2,aq}$ (cal · mol^{-1})[a]	$S^\circ_{2,aq}$ (cal · mol^{-1}K^{-1})[a]	V°_2 (cm^3 · mol^{-1})[a]	ξ	a (cm^3 · g^{-1})	b (cm^3 · K$^{0.5}$ · g^{-1})
Ar	3900[b]	14.30[b]	31.71[b]	0.0733	−7.6895	11.4657
Ne	4565[b]	16.74[b]	20.40[b]	0.5084	1.0014	4.7976
H_2S	−6673[b]	30.00[b]	34.90[b]	−0.2029	−13.4481	13.8821
CH_4	−8234[c]	20.99[c]	37.30[c]	−0.1196	−10.9926	14.4019
C_2H_4	19450[c]	28.70[c]	45.50[c]	−0.4499	−16.8037	18.8460
C_2H_6	−4141[d]	26.75[d]	51.20[d]	−0.6091	−16.3482	20.0628
C_3H_8	−2021[d]	33.49[d]	67.00[d]	−1.1471	−25.3879	28.2616
C_4H_{10}	99[d]	39.66[d]	82.80[d]	−1.6849	−33.8492	36.1457
C_6H_6	32000[d]	35.62[d]	83.50[d]	−1.9046	−39.1090	37.5421
H_3BO_3	−231540[e]	38.79[e]	39.60[f]	−1.0850	−3.5423	3.4693
HF	−71662[b]	22.50[b]	12.50[b]	0.1008	3.0888	−3.5714
SO_2	−71980[b]	38.70[b]	38.50[b]	−0.4295	−14.5223	14.3512

[a] Standard-state properties of aqueous species at 298.15 K, 1 bar, used in the estimation procedure; $\mu^\circ_{2,aq}$, chemical potential at infinite dilution; $S^\circ_{2,aq}$, partial molar entropy; V°_2, partial molar volume.
[b] Shock et al. (1989).
[c] Shock and Helgeson (1990).
[d] Amend and Helgeson (1997).
[e] Pokrovski et al. (1995).
[f] Hnědkovsky et al. (1995).

Our new EoS works well even for strongly dipolar molecules (HCl_{aq}, HF_{aq}) (Fig. 6) and for boric acid ($H_3BO_{3,aq}$) (Figs. 6 and 7). The latter is known to exhibit negative divergence of V°_2 and C°_{p2} near the critical point of H_2O, in contrast to most other nonelectrolytes (Hnědkovsky et al., 1995). Accordance between the experimental data and our model predictions is quite fair, especially considering that the empirical parameters for $H_3BO_{3,aq}$ were retrieved solely on the basis of known standard-states properties.

The performance of our new EoS is much better than that of our previous modified Redlich-Kwong EoS (Akinfiev, 1997),
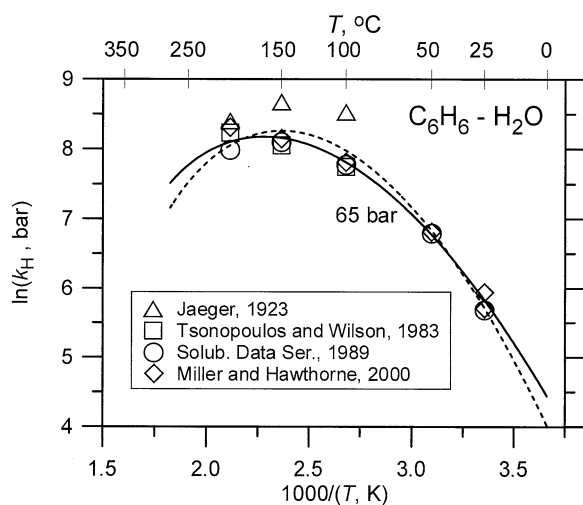

Fig. 4. Natural logarithm of Henry's constant ($\ln k_H$) for aqueous benzene at 65 bars, plotted against reciprocal temperature. Symbols correspond to experimental data. Solid curve is our equation of state (EoS) prediction, based on a least squares fit of the temperature dependence of k_H (parameters in Table 1). Dashed curve is our EoS prediction based solely on parameters retrieved from at standard-state conditions (Table 2).

which, for the example of H_2S, is accurate to ~0.15 $\log_{10}$ units but only at temperatures >100°C. A detailed comparison of our EoS with other published equations (see, e.g., the review by Sedlbauer and Majer, 2000) is the subject of a separate study. Here, we report a preliminary comparison of performance using data for $CO_{2,aq}$, $CH_{4,aq}$, H_2S_{aq} and $C_6H_{6,aq}$ over the range 0 to 300°C, as given by Sedlbauer and Majer (2000). It was found that the accuracy of our new EoS is comparable to that of the density model of Majer (1999) and to the models based on fluctuation solution theory (Plyasunov and Shock, 2001a, 2001b; Sedlbauer et al., 2000), and that it is better than the HKF model (Shock et al., 1989) and the EoS of Harvey et al. (1991). These differences in performance become particularly clear if the fitting procedure is based solely on experimental information for ambient temperatures. For example, Figure 8 compares the predictions for dissolved methane, $CH_{4,aq}$. The estimated deviations of the models of Sedlbauer et al. (2000), Plyasunov et al. (2000b), and our new EoS are approximately equal. However, the EoS of Sedlbauer et al. (2000) and Plyasunov et al. (2000b) use five and seven adjustable parameters, respectively, compared to the three parameters in our EoS. In the recent studies of Schulte et al. (2001) and Plyasunov and Shock (2001b), the HKF parameters for $CH_{4,aq}$ and some other nonelectrolytes were updated using recent experimental data on heat capacities and volumes, thereby improving the accuracy of the HKF model. Nevertheless, Plyasunov and Shock (2001b) stated that the extension of the revised HKF model to neutral species is theoretically unjustified, and they did not recommend its application in the near-critical and low-density regions of H_2O.

To illustrate an application of our EoS and to highlight how it intrinsically differs from the HKF model, we have calculated the temperature dependence of the equilibrium constant of the reaction of graphite with water
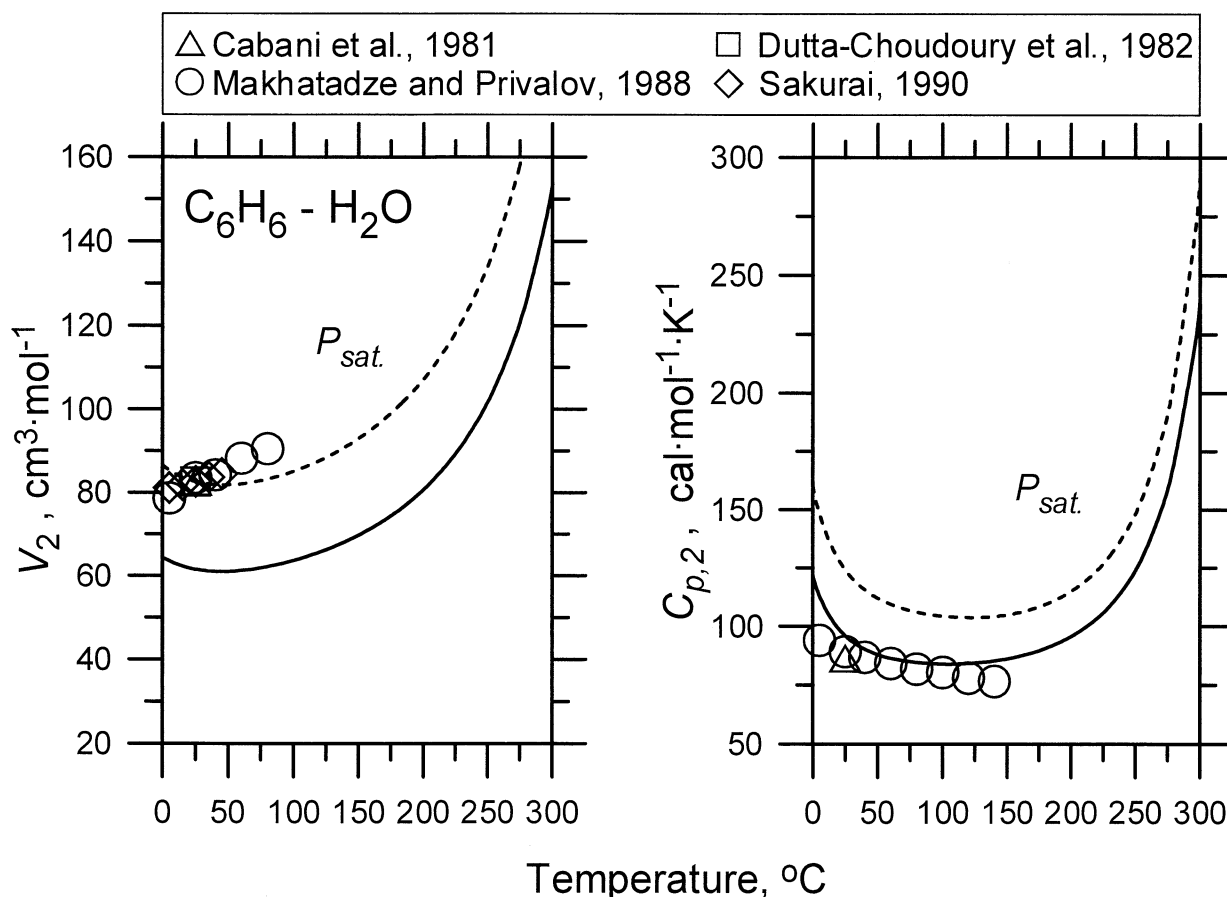
Fig. 5. Temperature dependencies of partial molar volumes (left) and apparent heat capacities (right) of dissolved benzene. Symbols represent to experimental data. Solid curves are our equation of state (EoS) predictions, based on a least squares fit of the temperature dependence of k_H (parameters in Table 1). Dashed curves are our EoS prediction based solely on parameters retrieved from $\mu_{2,aq}^{\circ}$, S_2° and V_2° at standard-state conditions (Table 2).

$$2C_{graphite} + 2H_2O \Leftrightarrow CO_2 + CH_4,$$
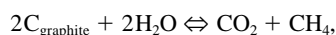
at a constant pressure of 280 bars (Fig. 9). Because of the widespread occurrence of graphite in the crust, this reaction plays an important role in buffering the compositions of hydrothermal and metamorphic fluids. It can be seen that differences between the predictions of the HKF model and our EoS are very large (up to 6 log units on a molal scale), especially at high temperatures. The noticeable discrepancies begin at $T > 350°C$, near the critical point, at which the density of water dramatically decreases. At high temperatures ($T > 550°C$), the predictions of our model (solid line in Fig. 9) steadily approach the limiting behaviour of the ideal gas mixture (dashed-dotted line), as they should: at $T = 700°C$ and $P = 280$ bars, the density of water is 0.068 g $\cdot$ cm^{-3}, and thus, the fluid mixture can be correctly described as an ideal mixture of ideal gases. Similar differences between the results of our EoS and those of the HKF EoS are also found at pressures up to ~2000 bars. We have chosen to display the 280-bar calculations in Figure 9 because although this pressure is not particularly relevant in high-temperature geological environments, it best illustrates the behaviour of our model with respect to the ideal gas limit.

The deviation of the HKF model from the low-density limiting behaviour is well known. We reiterate that Plyasunov and Shock (2001b), who most recently modified the HKF model, warned that its reliability is restricted to the high-density region, well removed from the critical point of water.

Depending on the geochemical system under investigation, differences in lg$K$ of the magnitudes shown in Figure 9 could easily cause large shifts in the calculated positions of mineral-fluid or homogeneous fluid reactions and hence lead to differences in the interpretation of geochemical processes. A related example is the buffering of oxygen fugacity by graphite:
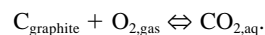
$$C_{graphite} + O_{2,gas} \Leftrightarrow CO_{2,aq}.$$

Figure 10 displays lgf_{O_2} defined by this equilibrium as a function of pressure and density at 500°C, for a constant activity of $CO_{2,aq}$ in the fluid equal to 1 (on a molal scale). As in Figure 9, it can be seen that our EoS predictions diverge increasingly from those of the HKF model as the density of water decreases. The differences in calculated lgf_{O_2} values for the same set of observations in a rock-water system (e.g., presence of modal graphite; aqueous CO_2 con-
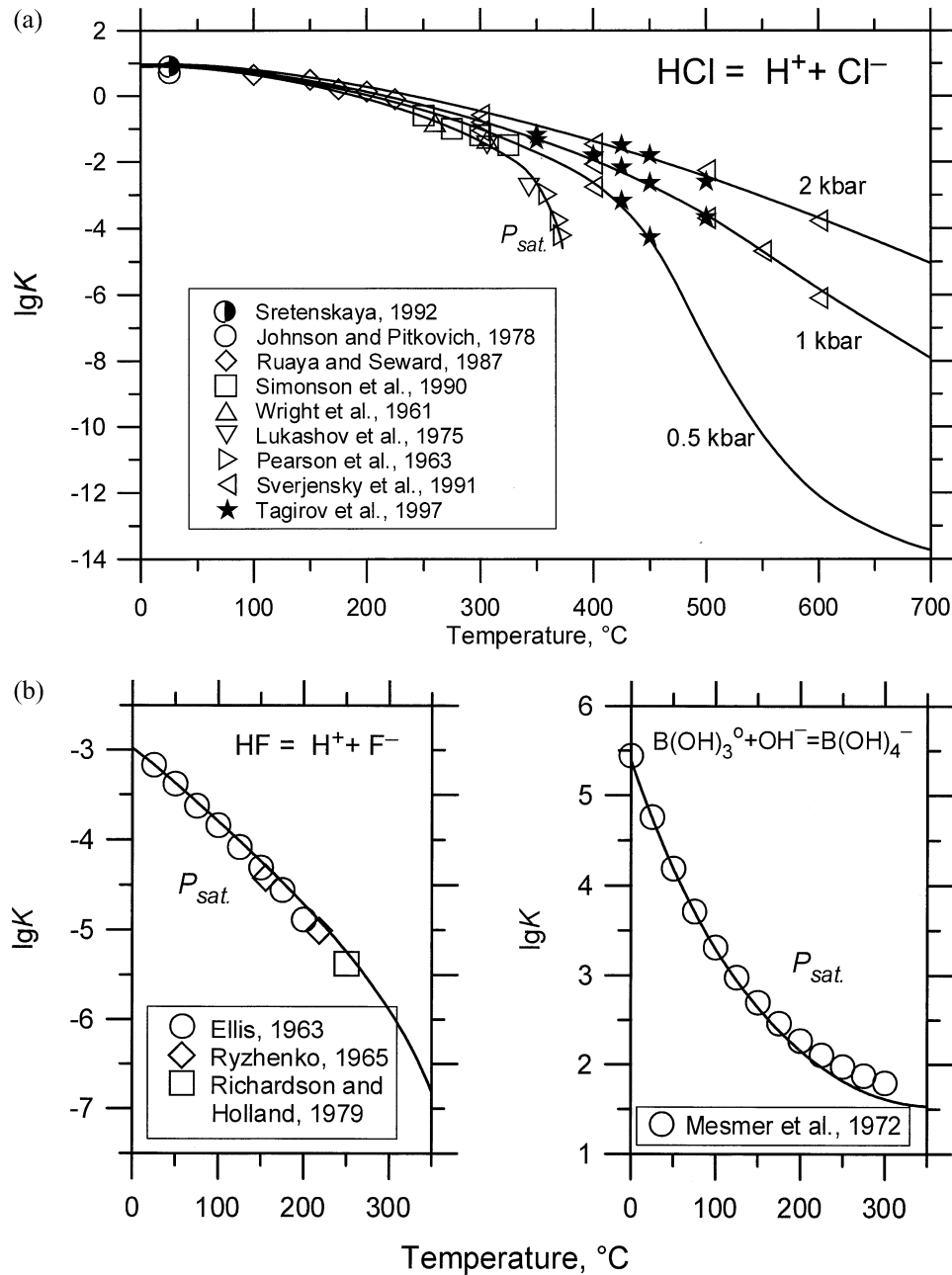
Fig. 6. Logarithm of equilibrium constants for acid dissociation reactions as a function of temperature at P_{sat}. Symbols represent experimental data; curves are theoretical predictions. Data for neutral species are taken from Tables 1 and 2 and calculated using our equation of state (EoS); ionic species are calculated using the Helgeson-Kirkham-Flowers EoS with data for F^-, Cl^-, and OH^- from SUPCRT92 (Johnson et al., 1992) and for $B(OH)_4^-$ from Pokrovski et al. (1995).

tent determined by fluid inclusion analysis) could obviously lead to different conclusions regarding redox-dependent mineral stability or metal solubility.

6. CONCLUDING REMARKS

Figures 1 to 3 demonstrate that our EoS provides good predictions of the entire set of investigated thermodynamic properties (chemical potential, entropy, molar volume, and heat capacity) of aqueous species at infinite dilution, over a wide P-T range encompassing the H_2O critical region. The EoS works well with both nonpolar (CO_2, N_2, etc.) and polar (NH_3, H_2S, etc.) neutral species.

In terms of the Henry constant, k_H, the standard deviations of the predictions with respect to the experimental data are <0.05 log_{10} units, and the standard deviation is ~0.08 log_{10} units in the case of H_2S. The accuracies of the calculated
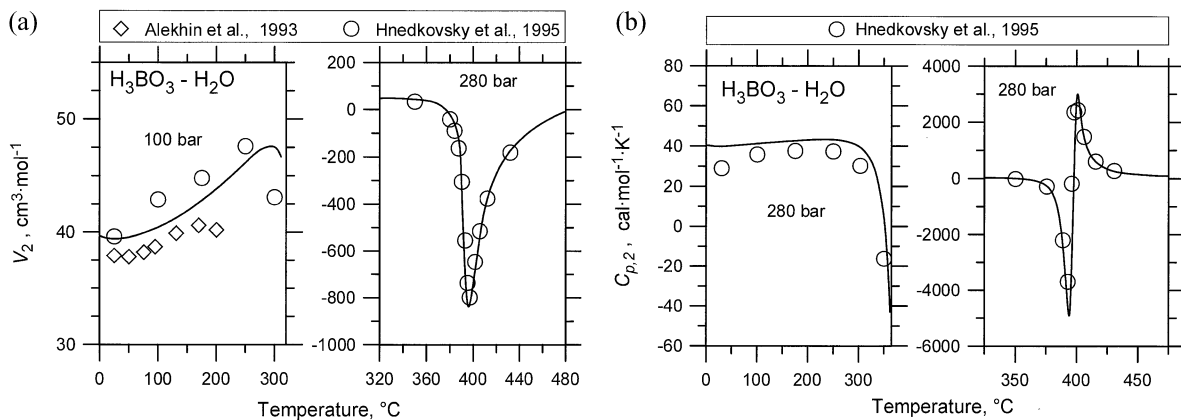
Fig. 7. (a) Volumes and (b) heat capacities of boric acid at subcritical (left) and supercritical (right) temperatures. Symbols denote experimental data. Solid curves are our equation of state predictions at infinite dilution (Eqn. 19 and 21 and model parameters in Table 2).

temperature dependencies of V_2° and C_{p2}° are good measures of the predictive capacity of the new EoS because the corresponding experimental data were not used in the estimation procedure.

In general, our model predictions for nonelectrolytes are more accurate than those of the HKF model in the near-critical region and in the supercritical, low-density region of H_2O. The differences in predictions can lead to very large differences in reaction properties when neutral species are involved (e.g., Figs. 9 and 10).

Our new EoS is formulated with the same standard state as the HKF model, which is highly successful for charged
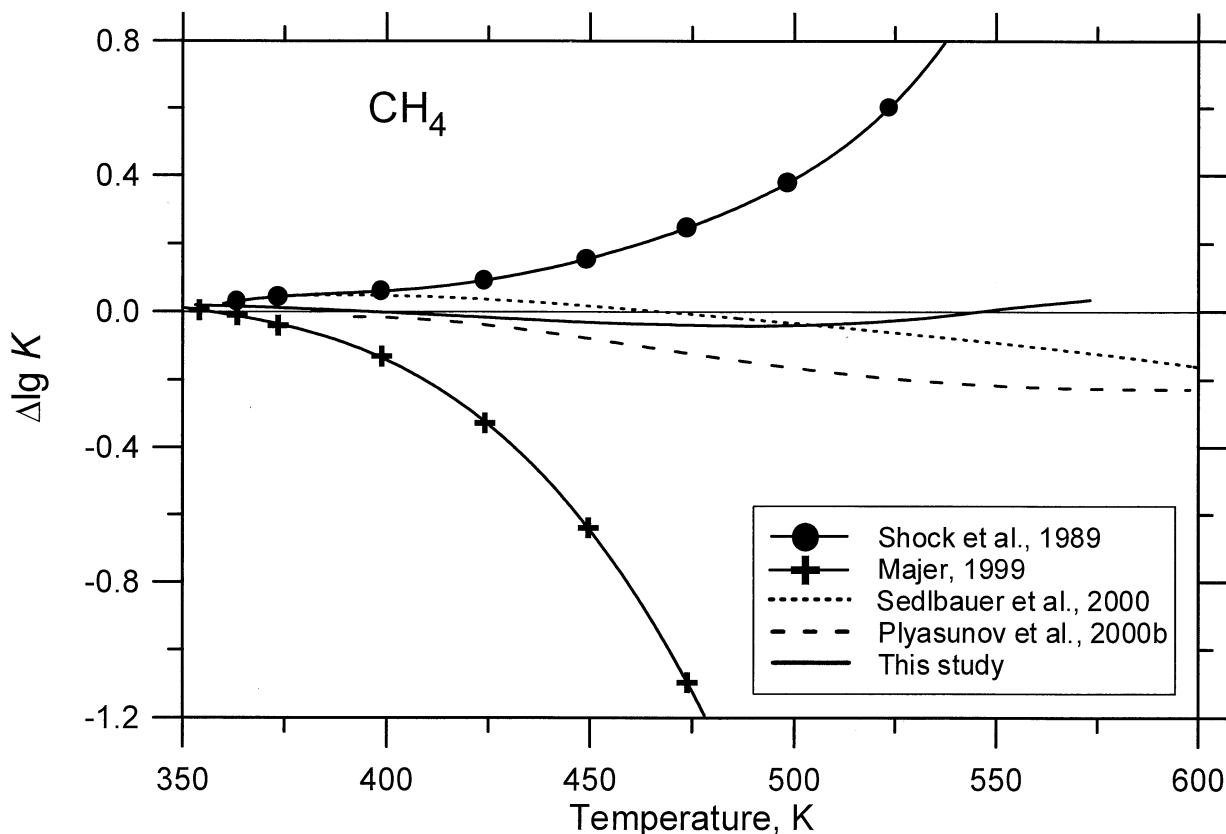

Fig. 8. Deviation between model and experimental values of the equilibrium constant for the aqueous dissolution of CH_4 ($\Delta \lg K \equiv \lg K_{\text{model}} - \lg K_{\text{experim}}$). The model fits are based only on experimental data at $T < 373$ K. With the exception of our equation of state, the data for this comparison were taken from Sedlbauer and Majer (2000).
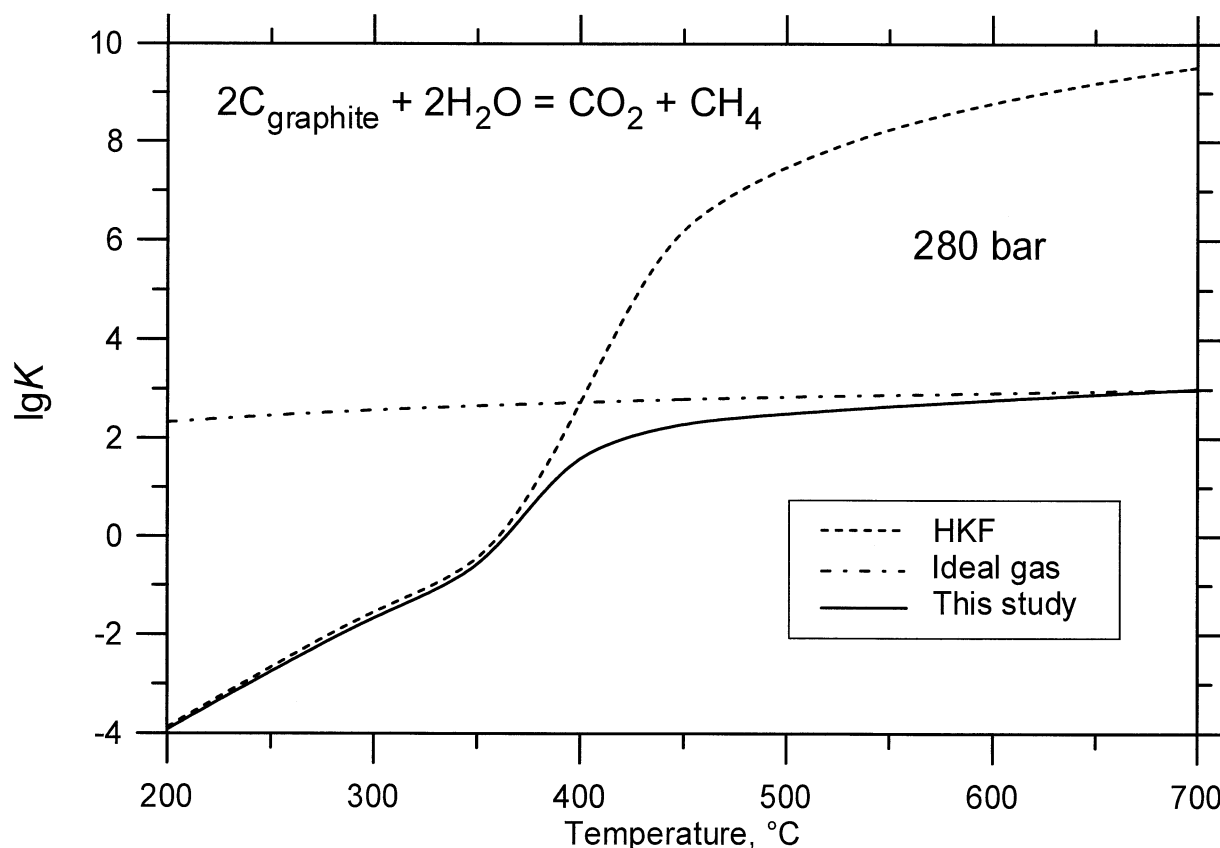
Fig. 9. Logarithms of the equilibrium constant (on a molal basis) for the reaction of graphite with water as a function of temperature at constant pressure of 280 bars. Dashed curve is the Helgeson-Kirkham-Flowers (HKF) equation of state (EoS) prediction with data for aqueous CO_2 and CH_4 from Shulte et al. (2001). Dashed-dotted curve represents an ideal mixture of the ideal gases H_2O_{steam}, CO_2, and CH_4. Solid curve is our EoS prediction. Thermodynamic properties of $C_{graphite}$, H_2O_{water}, H_2O_{steam}, and gaseous CO_2 and CH_4 were calculated using the SUPCRT92 package (Johnson et al., 1992). At high temperatures, our new EoS correctly approaches the limiting behaviour of the ideal gas mixture.

species, and it is fully compatible with the SUPCRT92 database of thermodynamic properties (Johnson et al., 1992). Therefore, there are no restrictions on applying our equation to reactions involving minerals, gases, and aqueous ions, in addition to uncharged species. For example, the predictions in Fig. 6 were calculated using our new EoS for the neutral species and the HKF equation for the charged species.

The performance of our new EoS is remarkably promising, considering that only three empirical constants need to be fitted to experimental data. Other published EoS perform equally well in some instances (e.g., Fig. 8), but these equations contain five or more empirical parameters. Nevertheless, the development of our EoS is far from complete. One of the goals of this paper is to call the attention of the geochemical community to the advantages of our approach so that it may be improved by common efforts. First, some discrepancies in C_{p2}°, especially at low temperatures and for large molecules (Fig. 5), must be reduced. Second, the EoS cannot be used automatically to describe aqueous electrolytes, because electrostatic interactions are not taken into account. To expand the applicability of the

EoS to electrolytes, its formalism must be interbred with an electrostatic approach. This possibility was recently demonstrated, in principle, using the example of $SiO_{2,aq}$ (Akinfiev, 2001).

From our point of view, the main limitation of the proposed EoS lies in the phenomenological character of the adopted temperature dependence of B_{12} (Eqn. 15). However, inasmuch as this intermolecular interaction coefficient has a well-defined physical meaning, it provides hope that a more rigorous formulation may be found in the future, free of empirical parameters.

The new EoS is available in the form of a computer code allowing calculations in units of calories or joules, in a format that is directly compatible with the SUPCRT92 database (Johnson et al., 1992). The code can be downloaded at no cost from the Web site www.geo.unibe.ch/people/akinfiev.
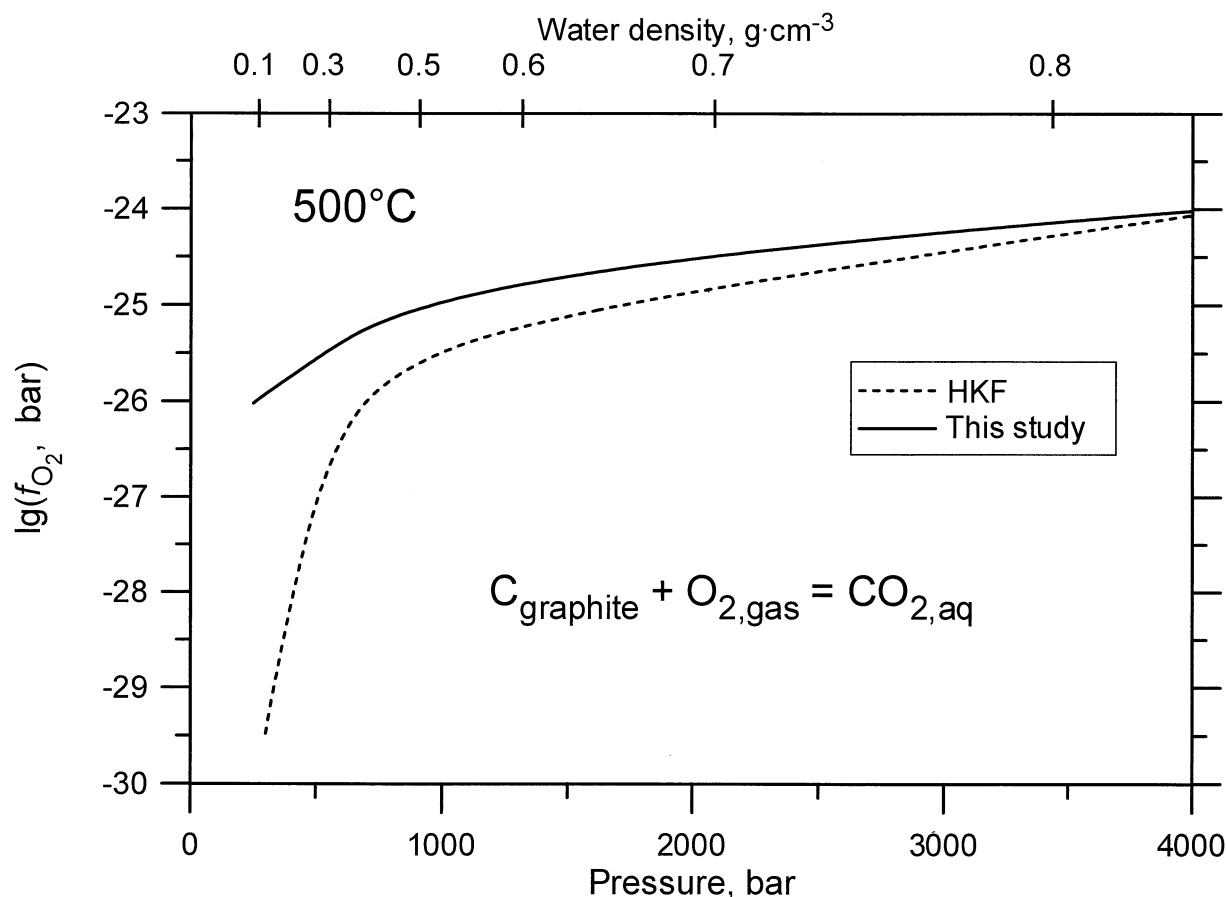
Fig. 10. Logarithms of oxygen fugacity vs. pressure as a result of the equilibrium $C_{graphite} + O_{2,gas} \Leftrightarrow CO_{2,aq}$ at 500°C and at constant activity of $CO_{2,aq}$ in the fluid equal to 1 (on a molal basis). Dashed curve is the Helgeson-Kirkham-Flowers (HKF) equation of state (EoS) prediction with data for aqueous CO_2 from Plyasunov and Shock (2001b). Solid curve is our EoS prediction. Thermodynamic properties for graphite and gaseous O_2 were calculated using the SUPCRT92 package (Johnson et al., 1992). The difference between the two models is most noticeable at low densities of H_2O, at which our EoS has correct limiting behaviour (Fig. 9).

Associate editor: E. H. Oelkers

REFERENCES

Akinfiev N. N. (1997) Thermodynamic description of H_2O-gas binary systems by means of Redlich-Kwong equation over a wide range of parameters of state. *Geochem. Intern.* **35**(2), 188–196.

Akinfiev N. N. (2001) Equation of state of SiO_{2aq} for description of silica dissolution at temperatures of 0–600°C and pressures of 1–1000 bar. *Geochem. Intern.* **39**, 1242–1244.

Alekhin O. S., Tsai S. V., Gilyarov V. N., Puchkov L. V., and Zarembo V. I. (1993) PVTX data in H_3BO_3-H_2O and NaB(OH)4-H_2O systems in the 298 - 573 K temperature range and the range of pressures from equilibrium to 80 MPa [in Russian]. *Zh. Prikl. Khimii.* **66**, 441–444.

Allred G. C. and Woolley E. M. (1981) Heat capacities of aqueous acetic acid, sodium acetate, ammonia and ammonium chloride at 283.15 K, 298.15 K, and 313.15 K: ΔC_p°. *J. Chem. Thermodyn.* **13**, 155–164.

Alvarez J., Crovetto R., and Fernandez-Prini R. (1988) The dissolution of N_2 and of H_2 in water from room temperature to 640 K. *Ber. Bunsengen. Phys. Chem.* B.92, S.935.

Amend J. P. and Helgeson H. C. (1997) Group additivity equations of state for calculating the standard molal thermodynamic properties of aqueous organic species at elevated temperatures and pressures. *Geochim. Cosmochim. Acta* **61**, 11–46.

Barbero J. A., McCurdy K. G., and Tremaine P. R. (1982) Apparent molal heat capacities and volumes of aqueous hydrogen sulfide and sodium hydrogen sulfide near 25°C: The temperature dependence of H_2S ionization. *Can. J. Chem.* **60**, 1872–1880.

Barbero J. A., Hepler L. G., McCurdy K. G., and Tremaine P. R. (1983) Thermodynamics of aqueous carbon dioxide and sulfur dioxide: Heat capacities, volumes and the temperature dependence of H_2O ionization. *Can. J. Chem.* **61**, 2509–2519.

Barta L. and Bradley D. J. (1985) Extension of the specific interaction model to include gas solubilities in high temperature brines. *Geochim. Cosmochim. Acta* **49**, 195–203.

Bazaev A. R., Skripka V. G., and Namiot A. Yu. (1977) Increase in water volume while dissolving methane [in Russian]. *Gazovaya promyshlennost'* **2**, 39.

Beattie J. A. (1955) Thermodynamic properties of real gases and mixtures of real gases. In *Thermodynamics and Physics of Matter*, (ed. F. D. Rossini **1**, 240–338. Princeton Univ. Press, Princeton, N.J.

Biggerstaff D. R. and Wood R. H. (1988a) Apparent molar volumes of aqueous argon, ethylene, and xenon from 300 to 716 K. *J. Phys. Chem.* **92**, 1988–1994.

Biggerstaff D. R. and Wood R. H. (1988b) Apparent molar heat capacities of aqueous argon, ethylene, and xenon at temperatures up to 720 K and pressures to 33 MPa. *J. Phys. Chem.* **92**, 1994–2000.

Cabani S., Gianni P., Mollica V., and Lepori L. (1981) Group contributions to the thermodynamic properties of non-ionic organic solutes in dilute aqueous solution. *J. Sol. Chem.* **10,** 563–595.

Carroll J. J., Slupsky J. D., and Mather A. E. (1991) The solubility of carbon dioxide in water at low pressure. *J. Phys. Chem. Ref. Data* **20,** 1201–1209.

Clarke E. C. W. and Glew D. N. (1971) Aqueous nonelectrolyte solutions. Part VIII. Deuterium and hydrogen sulfide solubilities in deuterium oxide and water. *Can. J. Chem.* **49,** 691–698.

Cramer S. D. (1984a) Solubility of methane in brines from 0 to 300°C. *Ind. Eng. Chem. Proc. Des. Dev.* **23,** 533.

Cramer S. D. (1984b) Oxygen solubility in brines. *Ind. Eng. Chem. Proc. Des. Dev.* **23,** 618.

Crovetto R. (1991) Evaluation of solubility data of the system CO_2 - H_2O from 273 to the critical point of water. *J. Phys. Chem. Ref. Data* **20,** 575–589.

Crovetto R. and Wood R. H. (1992) Solubility of CO_2 in water and density of aqueous CO_2 near the solvent critical temperature. *Fluid Phase Equil.* **74,** 271–288.

Crovetto R., Fernández-Prini R., and Japas M. L. (1982) Solubilities of inert gases and methane in H_2O and in D_2O in the temperature range of 300 to 600 K. *J. Chem. Phys.* **76**(2), 1077–1086.

Crovetto R., Wood R. H., and Majer V. (1991) Revised densities of $\{xCO_2 + (1 - x)H_2O\}$ with $x < 0.014$ at supercritical conditions. Molar volumes, partial molar volumes of CO_2 at infinite dilution, and excess molar volumes. *J. Chem. Therm.* **23,** 1139–1146.

Drummond S. E. (1981) *Boiling and Mixing of Hydrothermal Fluids: Chemical Effects of Mineral Precipitation.* Ph.D. thesis, Pennsylvania State University.

Dutta-Choudoury M. K., Miljevic N., and Hook A. V. (1982) Isotope effects in aqueous systems. 13. The hydrophobic interaction. Some thermodynamic properties of benzene/water and toluene/water solutions and their isotope effects. *J. Phys. Chem.* **86,** 1711–1721.

Ellis A. J. (1963) The effect of temperature on the ionization of hydrofluoric acid. *J. Chem. Soc.,* 4300–4304.

Ferry J. M. and Baumgartner L. (1987) Thermodynamic models of molecular fluids at the elevated pressures and temperatures of crustal metamorphism. *Rev. Mineral.* **17,** 323–366.

Gallagher J. S., Crovetto R., and Levelt Sengers J. M. H. (1993) The thermodynamic behaviour of the CO_2 - H_2O system from 400 to 1000 K, up to 100 MPa and 30% mole fraction of CO_2. *J. Phys. Chem. Ref. Data* **22,** 431–494.

Glushko V. P. (1981) *Thermal Constants of Substances: Directory in Ten Issues* [in Russian]. Issue 10, Part 1–2. Moscow, Academy of Sciences of the USSR, All-Union Institute of Scientific and Technical Information, Institute of High Temperatures.

Harvey A. H. (1996) Semiempirical correlation for Henry's constants over large temperature ranges. *AIChE J.* **42,** 1491–1494.

Harvey A. H. and Levelt Sengers J. M. H. (1990) Correlation of aqueous Henry's constants from 0°C to the critical point. *AIChE J.* **36,** 539–546.

Harvey A. H., Levelt Sengers J. M. H., and Tanger J. C., IV (1991) Unified description of infinite-dilution thermodynamic properties for aqueous species. *J. Phys. Chem.* **95,** 932–937.

Hill P. G. (1990) A unified fundamental equation for the thermodynamic properties of H_2O. *J. Phys. Chem. Ref. Data* **19,** 1233–1274.

Hnědkovsky L. and Wood R. H. (1997) Apparent molar heat capacities of aqueous solutions of CH_4, CO_2, H_2S, and NH_3 from 304 K to 704 K at 28 MPa. *J. Chem. Thermodyn.* **29,** 731–747.

Hnědkovsky L., Majer V., and Wood R. H. (1995) Volumes and heat capacities of $H_3BO_3(aq)$ at temperatures from 298.15 K to 705 K and pressures to 35 MPa. *J. Chem. Thermodyn.* **27,** 801–814.

Hnědkovsky L., Wood R. H., and Majer V. (1996) Volumes of aqueous solutions of CH_4, CO_2, H_2S, and NH_3 at temperatures from 298.15 K to 705 K and pressures to 35 MPa. *J. Chem. Thermodyn.* **28,** 125–142.

Jaeger A. (1923) Über die Löslichkeit von flüssigen Kohlenwasserstoffen in überhitztem Wasser. *Wasser Brennst. Chem.* **4,** 259.

Japas M. L. and Levelt Sengers J. M. H. (1989) Gas solubilities and Henry's law near the solvent's critical point. *AIChE J.* **35,** 705.

Johnson J. W., Oelkers E. H., and Helgeson H. C. (1992) SUPCRT92: A software package for calculating the standard molal thermodynamic properties of minerals, gases, aqueous species, and reactions from 1 to 5000 bars and 0° to 1000°C. *Comput. Geosci.* **18,** 899–947.

Johnson K. S. and Pytkowich R. M. (1978) Ion association of Cl^- with H^+, Na^+, K^+, Ca^{2+}, and Mg^{2+} in aqueous solutions at 25°C. *Am. J. Sci.* **278,** 1428–1447.

Jones M. E. (1963) Ammonia equilibrium between vapor and liquid aqueous phases at elevated temperatures. *J. Chem. Phys.* **67,** 1113–1120.

Kawazuishi K. and Prausnitz J. M. (1987) Correlation of vapor-liquid equilibria for the system ammonia-carbon dioxide-water. *Ind. Eng. Chem. Res.* **26,** 1482–1485.

Kertes A. S. Ed. (1989) *Solubility Data Series. IUPAC,* Pergamon Press, Oxford, UK.

Kishima N. (1989) A thermodynamic study on the pyrite-pyrrhotite-magnetite-water system at 300 - 500°C with relevance to the fugacity/concentraton quotient of aqueous H_2S. *Geochim. Cosmochim. Acta* **53,** 2143–2155.

Kishima N. and Sakai H. (1984) Fugacity - concentration relationship of dilute hydrogen in water at elevated temperature and pressure. *Earth Planet. Sci. Lett.* **67,** 79–86.

Kozintseva T. N. (1964) Solubility of hydrogen sulfide in water at elevated temperatures. *Geochem. Intl.* **1,** 1739–1754.

Levelt Sengers J. M. H. (1991) Solubility near the solvent's critical point. *J. Supercrit. Fluids* **4,** 215–222.

Levelt Sengers J. M. H. and Gallagher J. S. (1990) Generalized corresponding states and high-temperature aqueous solutions. *J. Phys. Chem.* **94,** 7913–7922.

Levelt Sengers J. M. H., Chang R. F., and Morrison G. (1986) In *Equations of State, Theories and Applications, ACS Symposium Series 300.* (eds. K. C. Chao, R. L. Robinson, Jr.), chap. 5. *Critical behaviour in fluids and fluid mixtures.* American Chemical Society: Washington, DC.

Lukashov Yu. M., Komissarov K. B., Golubev B. R., Smirnov S. N., and Svistunov E. R. (1976) An experimental investigation of the electrolytic properties of uni - univalent electrolytes at high parameters of state. *Therm. Eng.* **1,** 89–92.

Majer V. (1999) New approaches to calculation of Henry's constant of aqueous solutes at superambient conditions. In *High Pressure Chemical Engineering*, pp. 145–150. Proc. of Intern. Meeting of GVC-Fachausschuss Hochdruckverfahren Technik, Karlsruhe, Germany.

Makhatadze G. I. and Privalov P. L. (1988) Partial specific heat capacity of benzene and of toluene in aqueous solution determined calorimetrically for a broad temperature range. *J. Chem. Thermodyn.* **20,** 405–412.

Malinin S. D. (1979) *Physical Chemistry of Hydrothermal Systems With Carbon Dioxide* [in Russian]. Nauka Press, Moscow, Russia .

Mason E. A. and Spurling T. H. (1970) The virial equation of state. In *The International Encyclopedia of Physical Chemistry and Chemical Physics* (ed. J. S. Rowlinson), vol. 2, topic 10. The fluid state. Franklin Book Co.

Mesmer R. E., Baes C. F., Jr., and Sweeton F. H. (1972) Acidity measurements at elevated temperatures. VI. Boric acid equilibria. *Inorg. Chem.* **11,** 537–543.

Miller D. J. and Hawthorne S. B. (2000) Solubility of liquid organics of environmental interest in subcritical (hot/liquid) water from 298 K to 473K. *J. Chem. Eng. Data* **45,** 78–81.

Moore J. C., Battino T., Rettich T. R., Handa Y. P., and Wilhelm E. (1982) Partial molar volumes of gases at infinite dilution in water at 298.15 K. *J. Chem. Eng. Data* **27,** 22–24.

Namiot A. Yu. (1979) Specialities of solubility of gases in water at high temperatures [in Russian]. *Russ. J. Phys. Chem.* **53,** 3027–3033.

Namiot A. Yu. (1991) *Solubility of Gases in Water (Handbook)* [in Russian]. Nedra, Moscow, Russia.

O'Connell J. P. (1994) Thermodynamic and fluctuation solution theory with some applications to systems at near- or supercritical conditions. In *Supercritical Fluids for Application.* (eds. E. Kiran and J. M. H. Levelt Sengers), NATO ASI Series Applied Sciences, **273,** 191–229.

O'Connell J. P., Sharygin A. V., and Wood R. H. (1996) Infinite dilution partial molar volumes of aqueous solutes over wide ranges of conditions. *Ind. Eng. Chem. Res.* **35,** 2808–2812.

Olofsson G., Oshodi A. A., Qvarnstrom E., and Wadsö I. (1985) Calorimetric measurements on slightly soluble gases in water. Enthalpies of solution of helium, neon, argon, krypton, xenon, methane,

ethane, propane, 1-butane and oxygen at 288.15, 298.15 and 308.15 K. *J. Chem. Thermodyn.* **16,** 1041–1052.

Pearson D., Copeland C. S., and Benson S. W. (1963) The electrical conductance of aqueous hydrochloric acid in the range 300 to 383°. *Am. Chem. Soc. J.* **85,** 1047–1049.

Plyasunov A. V. (1991) The approximate computation of Henry's constants of non polar gases at water supercritical temperatures [in Russian]. *Dokl. Ak. Nauk SSSR.* **321,** 1071–1074.

Plyasunov A. V. and Zakirov I. V. (1991) Evaluation of thermodynamic properties of homogeneous H_2O - CO_2 mixtures at high temperatures and pressures [in Russian]. *Phys. Chem. Petrol. Sketches* **17,** 71–88.

Plyasunov A. V. and Shock E. L. (2000) Thermodynamic functions of hydration of hydrocarbons at 298.15 and 0.1 MPa. *Geochim. Cosmochim. Acta* **64,** 439–468.

Plyasunov A. V. and Shock E. L. (2001a) Estimation of the Krichevskii parameter for aqueous nonelectrolytes. *J. Supercrit. Fluids* **20,** 91–103.

Plyasunov A. V. and Shock E. L. (2001b) Correlation strategy for determining the parameters of the revised Helgeson-Kirkham-Flowers model for aqueous nonelectrolytes. *Geochim. Cosmochim. Acta* **65,** 3879–3900.

Plyasunov A. V., O'Connell J. P., and Wood R. H. (2000a) Infinite dilution partial molar properties of aqueous solutions of nonelectrolytes. I. Equations for partial molar volumes at infinite dilution and standard thermodynamic functions of hydration of volatile nonelectrolytes over wide ranges of conditions. *Geochim. Cosmochim. Acta* **64,** 495–512.

Plyasunov A. V., O'Connell J. P., Wood R. H., and Shock E. L. (2000b) Infinite dilution partial molar properties of aqueous solutions of nonelectrolytes. II. Equations for standard thermodynamic functions of hydration of volatile nonelectrolytes over wide ranges of conditions including the subcritical temperatures. *Geochim. Cosmochim. Acta* **64,** 2779–2795.

Pokrovski G. S., Schott J., and Sergeyev A. S. (1995) Experimental determination of the stability constants of $NaSO_4^-$ and $NaB(OH)_4^\circ$ in hydrothermal solutions using a new high-temperature sodium selective glass electrode—Implications for boron isotopic fractionation. *Chem. Geol.* **124,** 253–265.

Prausnitz J. M., Lichtenthaler R. N., and Gomes de Azeredo E. (1986) *Molecular Thermodynamics of Fluid-Phase Equilibria.* 2nd ed. Prentice Hall, New York.

Redlich O. and Kwong J. N. S. (1949) On the thermodynamics of solutions. V. An equation of state. Fugacities of gaseous solutions. *Chem. Rev.* **44,** 233–244.

Richardson C. K. and Holland H. D. (1979) The solubility of fluorite in hydrothermal solutions, an experimental study. *Geochim. Cosmochim. Acta* **43,** 1313–1325.

Ruaya J. R. and Seward T. M. (1987) The ion - pair constant and other thermodynamic properties of HCl up to 350°C. *Geochim. Cosmochim. Acta* **51,** 121–130.

Ryzhenko B. N. (1965) Determination of the dissociation constant of hydrofluoric acid and the conditions for replacement of calcite by fluorite. *Geochem. Intl.* **2,** 196–200.

Sakurai M. (1990) Partial molar volumes in aqueous mixtures of nonelectrolytes. IV. Aromatic hydrocarbons. *Bull. Chem. Soc. Jpn.* **63,** 1695–1699.

Schulte M. D., Shock E. L., and Wood R. H. (2001) The temperature dependence of the standard-state thermodynamic properties of aqueous nonelectrolytes. *Geochim. Cosmochim. Acta* **65,** 3919–3930.

Sedlbauer J. and Majer V. (2000) Data and models for calculating the standard thermodynamic properties of aqueous non-electrolyte solutes under hydrothermal conditions. *Eur. J. Miner.* **12,** 1109–1122.

Sedlbauer J., O'Connell J. P., and Wood R. H. (2000) A new equation of state for correlation and prediction of standard molal properties of aqueous electrolytes and nonelectrolytes at high temperatures and pressures. *Chem. Geol.* **163,** 43–63.

Shock E. L. and Helgeson H. C. (1990) Calculation of the thermodynamic and transport properties of aqueous species at high pressures and temperatures: Standard partial molal properties of organic species. *Geochim. Cosmochim. Acta* **54,** 915–945.

Shock E. L., Helgeson H. C., and Sverjensky D. A. (1989) Calculation of the thermodynamic properties of aqueous species at high pressures and temperatures: Standard partial molal properties of inorganic neutral species. *Geochim. Cosmochim. Acta* **53,** 2157–2183.

Simonson J. M., Holmes H. F., Busey R. H., Mesmer R. E., Archer D. G., and Wood R. H. (1990) Modeling the thermodynamics of electrolyte solutions to high temperatures including ion association. Application to hydrochloric acid. *J. Phys. Chem.* **94,** 7675–7681.

Sretenskaya N. G. (1992) The dissociation constants of hydrochloric acid from the electrical conductance data for HCl solutions in the water-dioxane mixtures [in Russian]. *Geokhimiya* 447–453.

Suleimenov O. M. and Krupp R. E. (1994) Solubility of hydrogen sulfide in pure water and in NaCl solutions, from 20 to 320°C and at saturation pressures. *Geochim. Cosmochim. Acta* **58,** 2433–2444.

Sverjensky D. A., Hemley J. J., and D'Angelo W. M. (1991) Thermodynamic assessment of hydrothermal alkali feldspar - mica - aluminosilicate equilibria. *Geochim. Cosmochim. Acta* **55,** 989–1004.

Tagirov B., Zotov A. V., and Akinfiev N. N. (1997) Experimental study of dissociation of HCl from 350 to 500°C and from 500 to 2500 bars: Thermodynamic properties of HCl(aq). *Geochim. Cosmochim. Acta* **61,** 4267–4280.

Tanger J. C. IV and Helgeson H. C. (1988) Calculation of the thermodynamic and transport properties of aqueous species at high pressures and temperatures: Revised equations of state for standard partial molal properties of ions and electrolytes. *Am. J. Sci.* **288,** 19–98.

Tiepel E. W. and Gubbins K. E. (1972) Partial molal volumes of gases dissolved in electrolyte solutions. *J. Phys. Chem.* **76,** 3044–3049.

Tsonopoulos C. and Wilson G. M. (1983) High-temperature mutual solubilities of hydrocarbons and water. Part I: Benzene, cyclohexane and *n*-hexane. *AIChE J.* **29**(6), 990–999.

Wong D. S. H. and Sandler S. I. (1992) A theoretically correct mixing rule for cubic equations of state. *AIChE J.* **38,** 671–680.

Wright J. M., Lindsay W. T., and Druga T. R. (1961) *The Behaviour of Electrolytic Solutions at Elevated Temperatures as Derived From Conductance Measurements.* USAEC Report WAPAD-TM-204.

APPENDIX

Derivation of Eqn. 9

A.$ Starting with the general expression for the fugacity of a gas (Prausnitz et al., 1986)

$$\ln f \equiv \ln P - \int_0^P \left(\frac{1}{P} - \frac{V}{RT} \right) dP = \ln P|_{P=0} + \frac{1}{RT} \int_0^P V dP, \tag{A1}$$

and using the virial Eqn. 8 for integration

$$P = \frac{RT}{V} + RT \frac{B}{V^2}, \tag{A2}$$

and as

$$\frac{\partial P}{\partial V}\bigg|_T = -\frac{RT}{V^2} - \frac{2RTB}{V^3}, \tag{A3}$$

we obtain

$$\int_0^P V dP = \int_\infty^V V \frac{\partial P}{\partial V} dV = -\int_\infty^V \left(\frac{RT}{V} + \frac{2RTB}{V^2} \right) dV = -$$

$$RT\ln V + RT\ln V\bigg|_{P=0} + \frac{2RTB}{V}. \tag{A4}$$

Because for an ideal gas $\ln(PV)|_{P \to 0} = \ln RT$, we then have

$$\ln f = \ln \frac{RT}{V} + \frac{2B}{V}. \tag{A5}$$

Taking into account that

$$f = P \cdot \varphi, \tag{A6}$$

where φ stands for the fugacity coefficient of the gas, we finally obtain for the pure gas

$$\ln\varphi = \frac{2B}{V} - \ln\frac{PV}{RT}. \tag{A7}$$

For the fugacity coefficient of the dissolved component of the binary mixture, φ_2, we obtain a similar expression (Prausnitz et al.,1986; see also section A.5 below):

$$\ln\varphi_2 = \frac{2}{V}(x_2B_2 + x_1B_{12}) - \ln\frac{PV}{RT}. \tag{A8}$$

Here, as customary, variables without indexes refer to the mixture as a whole, x_1 and x_2 denote mole fractions of the component in the mixture, B_2 is the virial coefficient of the pure component 2 (solute), and the virial cross-coefficient B_{12} characterizes interaction between the dissimilar molecules. At infinite dilution, $x_1 = 1$, $x_2 = 0$, f and V correspond to that of the pure solvent $f = f_1^°$ and $V = V_1^°$. Thus, Eqn. A8 can be rewritten

$$\ln\varphi_2^∞ = \frac{2}{V_1^°}B_{12} - \ln\frac{PV_1^°}{RT}. \tag{A9}$$

A.2. Low-Density Limit of the New EoS

The ξ-dependent part of Eqn. 19 is in fact

$$V_2^°\propto V_1^°(1 - \xi) + \xi RT\frac{1}{\rho_1^°}\frac{\partial\rho_1^°}{\partial P} = V_1^°(1 - \xi) - \xi RT\frac{1}{V_1^°}\frac{\partial V_1^°}{\partial P}, \tag{A10}$$

and at the low pressure limit, when $V_1^° \to \frac{RT}{P}$, Eqn. A10 becomes

$$V_2^° \propto V_1^°(1 - \xi) - \xi RT\frac{1}{V_1^°}\frac{\partial V_1^°}{\partial P} = V_1^°(1 - \xi) - \xi RT\frac{1}{V_1^°}\left[-\frac{(V_1^°)^2}{RT}\right]$$
$$= V_1^°, \tag{A11}$$

and thus, Eqn. A10 also tends to the ideal gas equation in the low-density limit.

A.3. Expressions for $S_{2,aq}^°$, $C_{p2}^°$, and $V_2^°$

To calculate values for $S_{2,aq}^°$, $C_{p2}^°$, and $V_2^°$ of the dissolved species (Eqn. 19 to 21), the analytical derivatives of $2T\rho_1^°\Delta B_\rho \equiv T\rho_1^°\left[a + b\left(\frac{10^3}{T}\right)^{0.5}\right]$ with respect to temperature and pressure can be derived directly from Eqn. 15:

$$\frac{\partial}{\partial T}(2T\rho_1^°\Delta B_\rho) = a\left(\rho_1^° + T\frac{\partial\rho_1^°}{\partial T}\right) + b\left(0.5\cdot10^{1.5}\cdot T^{-0.5}\cdot\rho_1^° + 10^{1.5}\cdot T^{0.5}\frac{\partial\rho_1^°}{\partial T}\right), \tag{A12}$$

$$\frac{\partial^2}{\partial T^2}(2T\rho_1^°\Delta B_\rho) = a\left(2\frac{\partial\rho_1^°}{\partial T} + T\frac{\partial^2\rho_1^°}{\partial T^2}\right) + b\left(-0.25\cdot10^{1.5}\cdot T^{-1.5}\cdot\rho_1^° + 10^{1.5}\cdot T^{-0.5}\cdot\frac{\partial\rho_1^°}{\partial T} + 10^{1.5}\cdot T^{0.5}\cdot\frac{\partial^2\rho_1^°}{\partial T^2}\right), \tag{A13}$$

$$\frac{\partial}{\partial P}(2T\rho_1^°\Delta B_\rho) = aT\frac{\partial\rho_1^°}{\partial P} + b\cdot10^{1.5}\cdot T^{0.5}\frac{\partial\rho_1^°}{\partial P}. \tag{A14}$$

A.4. Adjustable Parameters of the New EoS Derived From Thermodynamic Properties at Standard-State Conditions

Using values derived from Hill's (1990) EoS for H_2O at standard-state conditions (25°C, 1 bar): $\rho_1^° = 0.9970$ g $\cdot$ cm^{-3}, $\frac{\partial\rho_1^°}{\partial T} = -2.571\cdot10^{-4}$ g$\cdot$cm$^{-3}\cdot$K^{-1}, $\frac{\partial^2\rho_1^°}{\partial T^2} = -9.503\cdot10^{-6}g\cdot$cm$^{-3}\cdot$K^{-2}, $\frac{\partial\rho_1^°}{\partial P} = 4.511\cdot10^{-5}$ g$\cdot$cm$^{-3}\cdot$bar^{-1} , and $\ln(f_1^°,$bar$) = -3.4773$, we

obtain a set of linear equations to estimate the three empirical parameters of the proposed model, ξ, a, and b:

$$10.7013\cdot\xi + 0.9970\cdot a + 1.8260\cdot b = \frac{\mu_{2,aq}^° - \mu_g^°}{592.48} + 7.4938$$

$$11.8547\cdot\xi - 1.8290\cdot a - 1.5353\cdot b = S_{2,aq}^° - S_{2,g}^° + 20.0629$$

$$-16.9470\cdot\xi + 1.1184\cdot a + 2.0482\cdot b = V_2^° - 18.069$$

Here, as above, $\mu_{2,aq}^°$ (cal $\cdot$ mol^{-1}), $S_{2,aq}^°$ (cal $\cdot$ mol^{-1}), and $V_2^°$ (cm$^3\cdot$mol^{-1}) stand for molal properties of aqueous species at infinite dilution at standard-state conditions (25°C, 1 bar); and $\mu_g^°$ (cal $\cdot$ mol^{-1}) and $S_{2,g}^°$ (cal $\cdot$ mol$^{-1}\cdot$K^{-1}) correspond to the ideal gaseous component at 25°C.

A.5. Concentration Dependencies

In the case of finite concentrations of the dissolved component, the general equation for fugacity of dissolved component 2 (Prausnitz et al., 1986) is to be used:

$$\ln f_2 \equiv \ln P_2 - \int_0^P\left(\frac{1}{P} - \frac{V_2}{RT}\right)dP, \tag{A15}$$

where P_2 and V_2 are partial pressure and molar volume of the dissolved component, respectively. Because $P_2 = x_2P$, we can rewrite Eqn. A15 such that

$$\ln f_2 \equiv \ln x_2 + \ln P - \int_0^P\left(\frac{1}{P} - \frac{V_2}{RT}\right)dP = \ln x_2 + \ln f + \frac{1}{RT}\int_0^P(V_2 - V)dP, \tag{A16}$$

where variables without indexes correspond to the mixture as a whole.

The partial volume V_2 can be defined as (Beattie, 1955)

$$V_2 \equiv V + x_1\frac{\partial V}{\partial x_2}, \tag{A17}$$

where x_1 is the mole fraction of the solvent. Then, using the derivative from Eqn. A2

$$\left.\frac{\partial P}{\partial x_2}\right|_{V,T} = \frac{RT}{V^2}\cdot\frac{\partial B}{\partial x_2}, \tag{A18}$$

together with the chain Eulerian expression

$$\frac{\partial V}{\partial P}\cdot\frac{\partial P}{\partial x_2} = -\frac{\partial V}{\partial x_2}, \tag{A19}$$

we can finally represent Eqn. A16 in the form

$$\ln f_2 = \ln x_2 + \ln f + \frac{x_1}{V}\cdot\frac{\partial B}{\partial x_2}. \tag{A20}$$

Here, f is the fugacity of the mixture, V is the molar volume of the solution, and B may be calculated from the standard mixing rule (Beattie, 1955):

$$B = B_1x_1^2 + 2B_{12}x_1x_2 + B_2x_2^2. \tag{A21}$$

Combining Eqn. A20 with the derivative of Eqn. A21

$$\frac{\partial B}{\partial x_2} = 2B_2x_2 + 2B_{12}(x_1 - x_2) - 2B_1x_1, \tag{A22}$$

and using Eqn. 2, A6, and A7 for $\ln f$ in Eqn. A20, we finally obtain

$$\ln f_2 = \ln x_2 + \ln\frac{RT}{V} + \frac{2}{V}(B_{12}x_1 + B_2x_2), \tag{A23}$$

which is similar to Eqn. A8.